remote sensing

MDPI

Systematic Review

Retrieval of Multiple Variables from Hyperspectral Data: A PRISMA-Aligned Systematic Review of Classical Physics-Based Machine Learning and Hybrid Algorithms in Vegetation and Raw Materials Application Domains

Andrea Taramelli [1,2], Sara Liburdi [1,*], Alessandra Nguyen Xuan [2], Simone Mancon [3], Serena Sapio [1,4] and Emiliana Valentini [1,4]

[1] Department of Science, Technology and Society (STS), University School for Advanced Studies IUSS Pavia, Palazzo del Broletto, Piazza della Vittoria 15, 27100 Pavia, Italy; andrea.taramelli@iusspavia.it (A.T.); serena.sapio@iusspavia.it (S.S.); emiliana.valentini@cnr.it (E.V.)
[2] Institute for Environmental Protection and Research (ISPRA), Via Vitaliano Brancati 48, 00144 Roma, Italy; alessandra.nguyenxuan@isprambiente.it
[3] ARESYS s.r.l., Via Luigi Cadorna 66, 20055 Vimodrone, Milan, Italy; simone.mancon@aresys.it
[4] National Research Council of Italy, Institute of Polar Sciences, Via Salaria km 29,300, 00015 Montelibretti, Italy
* Correspondence: sara.liburdi@uniroma1.it

Highlights

What are the main findings?

- Machine learning and deep learning approaches dominate vegetation applications, while classical physics-based methods remain prevalent in raw materials, with hybrid models achieving the highest overall performance across domains.
- Across vegetation, mineral and methane mapping, insufficient standardization of accuracy metrics and incomplete methodological reporting represent the main sources of bias rather than algorithmic limitations.

What are the implications of the main findings?

- Hybrid physics-informed machine learning approaches emerge as the most promising pathway to ensure robustness, transferability and operational readiness for upcoming hyperspectral missions.
- The results provide evidence-based guidance for algorithm selection and development aligned with user requirements of current and future hyperspectral missions, such as PRISMA, CHIME, SBG and IRIDE.

Abstract

Hyperspectral (HSI) remote sensing has emerged as a transformative technology for Earth Observation, enabling detailed assessments across different domains. The current PRISMA-aligned systematic review aims to compare classical physics-based algorithms with emerging machine learning (ML), deep learning (DL) and hybrid approaches across two relevant application domains (vegetation and raw materials), analyzing over 350 peer-reviewed studies (194 after the screening) sourced from Scopus and Web of Science and accessed in July 2025. Specific domain-related studies have been considered, excluding duplicates and studies not strictly related to HSI. Risk of bias was assessed qualitatively based on different criteria. The efficiency of the techniques was analyzed by comparing the accuracy metrics reported in the studies. The heterogeneity of the evaluation metrics used across the different categories of the studies and the underrepresentation of some application domains is the final baseline of the work. The results were synthesized, grouping by application

Academic Editor: Zhenwei Shi

Received: 5 January 2026
Revised: 16 February 2026
Accepted: 26 February 2026
Published: 5 March 2026

domains and algorithm category: ML and DL models dominate vegetation applications, and physics-based methods remain prevalent in raw materials. Hybrid models achieve the highest performances across all domains. This review highlights the importance of the hyperspectral operational requirements identified for upcoming missions (CHIME, SBG and IRIDE) and points out the opportunity for algorithm development.

Keywords: hyperspectral data; canopy water content; chlorophyll content; mineral mapping; methane mapping; hyperspectral missions; raw materials; vegetation

1. Introduction

Hyperspectral remote sensing has transformed how we observe and understand Earth, offering a window into its radiometric response complexity through hundreds of contiguous bands. This extraordinary level of detail enables applications ranging from raw material exploration [1] and vegetation biophysical assessment [2] to mapping atmospheric gases like methane [3]. Products derived from hyperspectral imaging are essential for tackling pressing challenges like climate change, sustainable resource management, and ecosystem conservation. Despite its remarkable capabilities, unlocking the full potential of hyperspectral data is far from straightforward [4]. Classical/physics-based (C/PB) algorithms, such as Spectral Angle Mapper (SAM), have long served as the backbone of hyperspectral data analysis. While effective for basic tasks, these methods often falter when confronted with the increasing volume, variety, and complexity of new hyperspectral datasets. This is highlighted by the advent of new hyperspectral missions: (I) Copernicus Hyperspectral Imaging Mission for the Environment (CHIME), developed by the European Space Agency as part of the Copernicus programme; (II) PLATiNO hyperspectral constellation of the IRIDE Earth Observation programme (a constellation of constellations funded through the Italian National Recovery and Resilience Plan); and (III) NASA's Surface Biology and Geology (SBG) mission. The relevance of these imminent missions lies in their design to yield operational, user-driven, and higher-level products. Notably, CHIME will furnish an operational mapping of vegetation traits and raw materials domains, derived from a preliminary user needs analysis. The mission outcomes will support food security, particularly in the domains of soil and vegetation variable assessment and mineral resource exploration. The SBG mission will be focused on global surface composition, with the aim of enabling supporting applications through an increased revisit frequency, particularly for mineral mapping and land monitoring. Finally, the IRIDE-PLATiNO will contribute high-resolution imaging capabilities, within a multi-mission system architecture, to obtain dynamic products, mainly related to land cover and land use. These missions highlight the need for robust, transferable and physically consistent algorithmic solutions.

It is imperative to emphasize that hyperspectral data analysis is accompanied by numerous challenges, which necessitate the development of sophisticated retrieval algorithms and an in-depth data examination and evaluation. The high dimensionality of hyperspectral imagery (HSI) gives rise to spectral collinearity, noise sensitivity and mixed-pixel effects, thereby rendering feature extraction and model generalization more difficult. Additionally, scene variability, atmospheric correction uncertainties and sensor-specific artefacts further exacerbate cross-sensor transferability. Furthermore, the escalating volume and intricacy of HSI produced by forthcoming missions necessitate scalable, reproducible and physically consistent models [5–8]. Machine learning (ML) offers tools to deal with these large and diverse datasets but can also be used to uncover complex patterns and relationships within them. Furthermore, ML algorithms have demonstrated their potential to address the shortcomings of classical methods, such as sub-pixel analysis algorithms, like the Linear Spectral Mixture Analysis (LSMA) or spectral matching (SM) [9]. Moreover, hybrid approaches that integrate ML with C/PB methodologies further enhance analytical precision and adaptability, paving the way for more robust solutions [10,11]. The current and upcoming challenges facing HIS analysis delineate the need for a systematic comparison of C/PB, ML and hybrid methods. This will help to explain how these algorithms, operating in isolation or in combination, can overcome these challenges.

This review sets out to understand which category of algorithms is the most efficient and suitable for hyperspectral data analysis considering C/PB algorithms, ML algorithms and hybrid (ML + C/PB) models. The aim is to identify existing gaps and opportunities, aligning them with the user needs of future hyperspectral missions, like CHIME and PLATiNO, providing a comprehensive overview of current methodologies [5,7]. This study focuses on two application domains: vegetation biophysical assessment and raw materials exploration. The selection of these two application domains is underpinned by two considerations. Firstly, these are considered the most relevant in the context of the current policy framework [7]. In particular, in the raw materials domain, included are strategic priorities related to industrial competitiveness, supply chain resilience, and strategic autonomy and security of resources. Regulatory frameworks, such as the Critical Raw Material Act (CRMA), explicitly identify a set of critical and strategic materials, which are essential in the context of the green and digital transition [12]. The Global Methane Pledge calls for a reduction in methane emissions as a short-term priority, requiring the capability to detect, map and analyze methane emissions, in particular from localized source points [13]. Although mineral and methane mapping are very different physical phenomena, they share common methodological challenges related to spectral discrimination, noise sensitivity, spatial heterogeneity and the need for robustness under operational conditions. For this reason, they are both considered in the raw materials domain in this work. In parallel, the vegetation domain is primarily related to climate adaptation, biodiversity protection and ecosystem resilience policies from a broader perspective to food security [14]. Schiavon et al. [7] collected the requirements from a user's communities to analyze the potential of hyperspectral satellites for responding to their needs. Most of these requirements were related to agriculture and ecosystem assessment. Despite this, these application domains show gaps due the current technical limits in hyperspectral data processing [7]. Secondly, both application domains are deemed the most suitable for further study and investigation given prevailing user requirements, mission objectives and the availability and focus of hyperspectral data. Furthermore, these domains are also included in CHIME's Mission Requirements Document [15]. In fact, this future Copernicus hyperspectral mission aims to satisfy the large community of users and address many needs in two main application domains, sustainable agriculture and food security, also including biodiversity protection, forest vegetation and related environmental degradation and hazards; the second one is raw materials, including, in particular, mine environment management [16]. The work of Berger et al. [17] systematically linked, for the first time in the European Union (EU), land-related agricultural and environmental policies to EO-derived variables that can be generated from upcoming satellite missions in the next ten years, such as CHIME. In this work, the authors analyzed the current Technologic Readiness Level (TRL) reached for each remotely sensed variables with proven added values, such as mineral abundances and compositions, leaf pigment content and vegetation water content, which support the potential for targeting critical raw materials and achieving the EU's biodiversity objectives and greenhouse gas emission reduction target, respectively. They revealed that it will be crucial to improve scientific algorithms and enhance the accuracy of the cited variables to develop mature products tailored to stakeholders and policymakers.

The analysis starts from the evaluation of user requirements considering the current and new hyperspectral missions' potential to implement algorithm innovations. Ultimately, this review aims to guide the hyperspectral research community toward scalable, innovative, and user-focused solutions that meet the challenges of a multi-satellite mission [12].

2. Background on Hyperspectral Data and Missions

2.1. Hyperspectral Data Background

Initiatives such as the European Critical Raw Material Act (CRMA) [12], Paris Agreement [18], and European Sustainable Agenda [19] provide the framework to underline and promote improvements in current technologies and methodologies related to the Earth Observation domain applied to environmental monitoring [7]. Hyperspectral imaging (HSI) remote sensing technology provides innovations, collecting surface reflectance information in multiple and continuous wavebands [20]. The potential of hyperspectral data is related to their application in different fields, such as raw material mapping, vegetation biophysical and biodiversity assessment and GHG mapping (e.g., methane). The strength of this type of data is related to the spectral resolution: hundreds of contiguous bands, comprising the spectral range between VNIR-SWIR from 400 to 2500 nm [21–23]. These types of characteristics can be used to better analyze the spectral composition of pixels, capturing detailed spectral information across the bands and enabling the identification and analysis of materials and processes with unmatched precision.

HSI can be acquired using different platforms: (1) satellites [24], (2) airborne [25], (3) Unmanned Aerial Vehicles (UAVs) [26] and (4) field instruments such as field spectroradiometers [27]. Unlike traditional multispectral systems, which divide the electromagnetic spectrum into a few broad bands, HSI resolves hundreds of narrow, contiguous bands, spanning a wide spectral range.

For this study, the focus is mainly on the Visible–Near Infrared (VNIR) range (400–1000 nm) and the Shortwave Infrared (SWIR) range (1000–2500 nm), which are both critical for numerous environmental and resource-based applications [28]. Table 1 provides a non-exhaustive summary of the most relevant spectral ranges for the two application domains selected in this review [29].

Table 1. Spectral features relevant for the application domain. Several products have been identified for each domain and are defined as "High Priority Products" or "Additional products", according to their classification in CHIME's Mission Requirements Document.

Application Domain	Spectral Range (nm)	Spectral Region	High Priority Products/Additional Products
Vegetation biophysical assessment	670, 710–730	Red Band, Red-Edge	Canopy Chlorophyll Content
	950–970, 1150–1260, 1450, 1950, 2250	NIR, SWIR	Canopy Water Content
Raw Materials	400–1000, 1000–2500, 8000–12,000	VNIR, SWIR, LWIR	Minerals (e.g., Fe-bearing minerals, Clay minerals, Carbonates, Silica)
	1650–2350	SWIR	Methane

2.2. Hyperspectral Missions Overview

This study leverages a diverse set of hyperspectral data sources, which comprise operational, decommissioned, and planned missions, across satellite, airborne, and UAV platforms. These platforms provide unique combinations of spatial, spectral, and temporal characteristics, enabling their application in different domains. Table 2 reports the most commonly used hyperspectral sensors, including information on the status of the mission and technical characteristics of sensors.

Table 2. Most commonly used and studied hyperspectral sensors: missions status with technical specifications (partially based on [7]).

Hyperspectral Mission/Platform and Owner	Type	Status and Year of Launch	Spatial Resolution	Revisit Time	Spectral Bands	Spectral Range (nm)	Spectral Resolution (nm)
PRISMA, HyperSpectral Precursor of the Application Mission (ASI-Italy)	Satellite	Operational (2019)	30 m	29 days On-Demand	66 VNIR-174 SWIR	400–2500	~12 nm
EnMAP (DLR-GFZ Germany)	Satellite	Operational (2022)	30 m	27 days	244	420–2450	6.5 nm (VNIR), 10 nm (SWIR)
EMIT (Nasa-USA)	Spaceborne (ISS)	Operational (2022)	60 m	Targeted areas for dust regions	285	380–2500	7.5 nm
DESIS (DLR-Germany)	Spaceborne (ISS)	Operational (2018)	30 m	On demand	235	402–1000	~2.55 nm
Hyperion (EO-1) (Nasa-USA)	Satellite	Decommissioned (2017)	30 m	16 days	70 VNIR-150 SWIR	426–2395	~10 nm
CHIME, Copernicus Hyperspectral Imaging Mission for the Environment (ESA-Europe)	Satellite	Planned (2028)	20–30 m	12–15 days	400+ (Planned)	400–2500	~10 nm (planned)
SBG, Surface Biology and Geology (Nasa-USA)	Satellite	Planned (2027–2028)	30 m	3 days	300+ (Planned)	380–2500	5–10 nm (targeted)
IRIDE, Hyperspectral constellation (PLATiNO) (ASI-ESA Italy-)	Satellite	Planned (2025–2026)	5 m PAN, 21 m SPOTLIGHT, 31 m	27 days	60 VNIR-256 SWIR	400–2500	10 nm (targeted)
AVIRIS (Nasa-JPL USA)	Airborne	Operational (1980s updated versions)	4–20 m	On demand	224 VNIR	380–2500	5–10 nm
HyMap (Commercial)	Airborne	Operational (1990s ongoing)	5–10 m	On demand	128	400–2500	15 nm
Specim FX17 (Specim-Finland)	UAV	Operational (2018)	0.5–2 m	On demand	224 SWIR	900–1700	8 nm

2.3. Hyperspectral Data: Gaps and User Requirements

Despite the potential of HSI, there are notable gaps between the capabilities of current missions and the operational needs expressed by diverse user communities [7]. Research conducted by the Italian Copernicus User Forum (CUF) [7] and the SBG science community (Surface Biology and Geology) [30] has identified high-priority needs for improved spatial resolution ($\leq$30 m), frequent revisit times ($\leq$2 weeks), and better exploitation of the VNIR-SWIR spectral range (400–2500 nm). Related to this, recent studies, such as those conducted for ESA's CHIME mission, underscore the importance of aligning mission planning and algorithm development with specific user requirements [15]. As shown in Figure 1, the current operational satellite sensors are unable to fully meet user requirements. Whilst UAV and airborne-based sensors can satisfy the requested spatial resolution, their number of bands is limited, and acquisition is only on demand. Conversely, the satellite sensors currently in orbit are close to meeting the requirements, both in terms of spatial resolution (almost always 30 m) and temporal resolution. Future satellite missions (i.e., CHIME and PLATiNO-IRIDE) will fully meet user demands, increasing the spatial resolution and the number of bands [17].

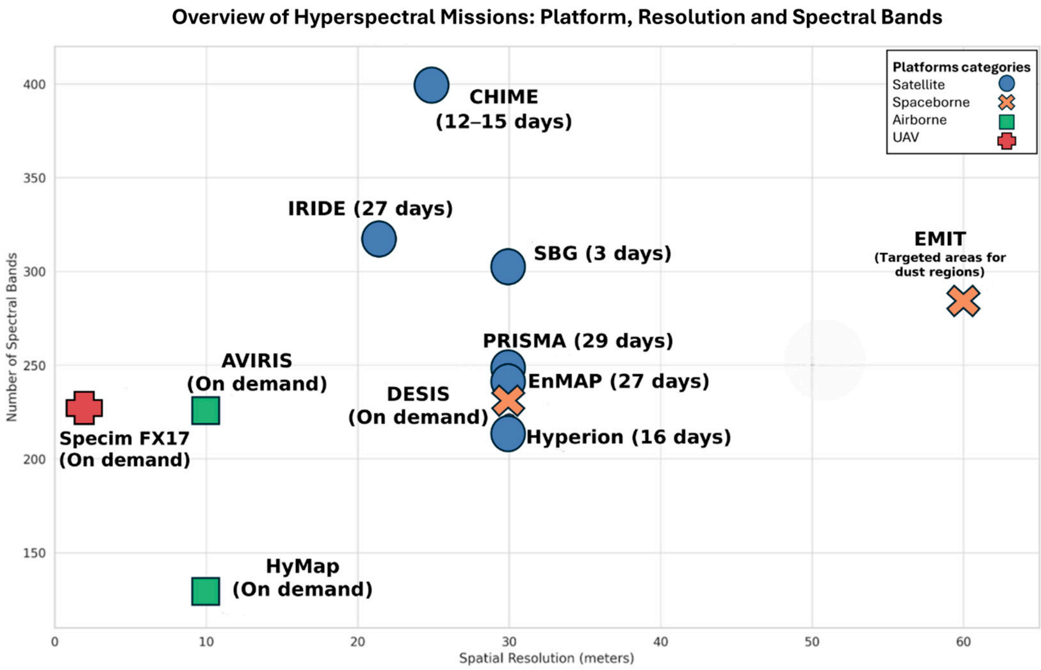

Figure 1. Most commonly used and studied hyperspectral sensors, distributed per number of spectral bands and spatial resolution. The symbols represent the type of platform, and, in brackets, the revisit time is reported.

These gaps, ranging from limited spatial resolution and temporal revisit time to underutilized spectral ranges (Figure 1), highlight the need for a concerted effort to enhance (1) data processing algorithms, (2) multi-mission synergy and (3) product retrieval [16]. Central to addressing these gaps is a user-centric approach that incorporates feedback from diverse stakeholders.

3. Algorithmic Framework for Hyperspectral Data

3.1. Algorithms for Hyperspectral Data Analysis in Different Application Domains

Regarding the development of data processing algorithms, user requests are different according to different applications [4]. Simple C/PB methodologies, such as Matched Filtering (MF) [31] and Continuum Removal [32], are computationally efficient and well-suited for specific, well-characterized applications but often struggle with high-dimensional data and overlapping spectral features. ML approaches, including Random Forests, Support Vector Machines (SVMs), and deep learning architectures like Convolutional Neural Networks (CNNs) or Mixture Density Networks (MDNs), offer the flexibility to handle complex datasets and extract nuanced patterns [11]. Recent deep architectures, specifically designed for hyperspectral image classification and segmentation, further confirm this trend, by combining multi-scale spectral–spatial encoding with attention mechanisms. Examples include multiarea target attention networks for classification, multi-scale convolutional and multi-attention models, and recent semantic segmentation frameworks such as SegHSI, which achieve accurate pixel-wise labeling with limited annotated samples [33]. Although these methods are not all directly applied to the specific products considered in this review, they illustrate the rapid evolution of deep learning-based HSI processing and point to algorithmic directions that could benefit future HPP retrievals. However, they rely heavily on the availability of large, high-quality training datasets, which are often scarce in the hyperspectral domain. A key contribution of this review lies in its focus on bridging the gaps identified in recent user requirement studies. The high number of available and future hyperspectral missions, and so the increasing number of data, will be a valuable opportunity to better investigate the multi-mission synergy and the requirements from user communities so that all services and specifications can be developed. This strategy can satisfy the three main user requirements related to hyperspectral data: higher spectral resolution, higher spatial resolution, higher temporal resolution related to revisit time [7]. Some of these gaps will be filled partially by new hyperspectral missions but also through synergy with multispectral and radar missions [34,35]. Such synergies also enable the development of specific algorithms, which are fundamental for ensuring interoperability across missions [16].

To advance in Earth Observation technologies, it is important to match the technical requirements on the specific thematic area with user requirements. Considering the future CHIME mission, the main data products related to the exploitation of hyperspectral data are provided at Level-2A (geometrically corrected and in surface reflectance). In addition to these, there are a set of Higher-Level Data Products that will be a part of the mission services offered by the EO to insert it in the downstream industry for business development. Inserted in Higher-Level Data Products, there are High-Priority Products (HPPs) (e.g., leaf and canopy chlorophyll content and canopy water content) for the vegetation application domain or, in the raw materials context, the composition and abundance of non-renewable raw materials (mainly minerals). Another additional product is large gas leakage detection, not an HPP, but a potential one, all of them leveraged on a specific spectrum portion [15].

For example, in the CHIME mission, HPPs are a set of higher-level products proposed to users as a part of the mission catalogue or services offered by the program. There are many different proposed HPPs for the CHIME mission, divided by application domains. In this review, the HPPs and the additional products considered are related to two of these domains: vegetation and raw materials (mineral mapping) [7,17,26,29].

3.2. Conceptual Differences Between AI, ML, DL, C/PB, and Hybrid

All the algorithms mentioned in the previous paragraph have been defined as C/PB or as ML techniques [24]. To fully understand the comparative framework developed in this review and the conceptual differences between algorithm classes, Table 3 reports the definition of Artificial Intelligence (AI), machine learning (ML), deep learning (DL), classical/physics-based (C/PB) algorithms and hybrid models, highlighting the strength and the limitations of each category [4,9].

Table 3. Algorithm categories description: definition, strengths and limitations of artificial intelligence, machine learning, deep learning, classical/physics-based and hybrid models.

Category	Definition	Key Methods	Strengths	Limitations
Artificial Intelligence (AI)	Development of systems capable of performing tasks requiring human intelligence, combining symbolic and data-driven approaches.	Symbolic AI, Expert Systems, ML	Combines reasoning and learning; general-purpose intelligence framework	Conceptual umbrella; not directly operational
Machine Learning (ML)	Subset of AI; algorithms that learn patterns from data to enable predictive or descriptive modeling.	Supervised, Unsupervised, Semi-supervised, Active, Transfer Learning	Flexible, adaptive, effective on noisy and high-dimensional data	Requires labeled data and tuning; can struggle with physical interpretability
Deep Learning (DL)	Subset of ML; multi-layer neural networks for hierarchical feature learning from raw data.	CNNs, RNNs, autoencoders, Transformers	Learns complex hierarchical features; high automation of feature extraction	High computational cost; needs large datasets

Table 3. *Cont.*

Category	Definition	Key Methods	Strengths	Limitations
Classical/Physics-based Algorithms	Algorithms based on deterministic physical models describing radiation-substrate interactions.	RTMs, MF, SAM, Linear/Non-linear Unmixing	Physically interpretable; transferable across conditions	Limited in handling non-linear relations; computational cost for RTMs
Hybrid Models	Models integrating physical constraints into ML/DL frameworks.	Physics-guided NN, Hybrid inversion (RTM + ML), ML corrections of physical outputs	Combines physical consistency with learning flexibility; improves generalization and uncertainty quantification	Requires careful integration design; still emerging in operational EO

In considering these categories, particular emphasis should be placed on the hybrid model, which involves the incorporation of physical constraints within machine learning and deep learning frameworks. Figure 2 provides a conceptual scheme to better clarify the interconnection and relationship between AI, ML, DL, C/PB and hybrid models.

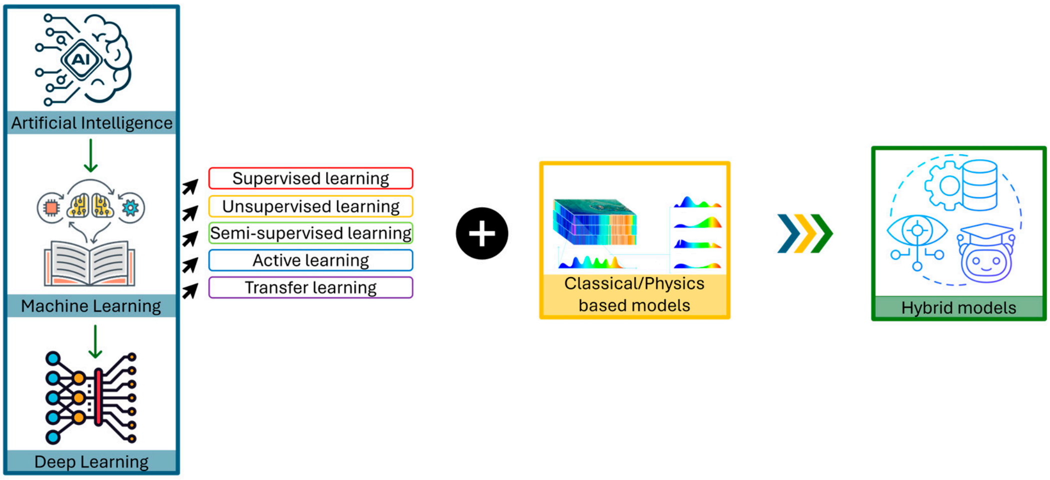

Figure 2. Conceptual scheme linking AI/ML learning framework (blue), classical/physics-based models (yellow) and their fusion into hybrid models (ML + C/PB) (green).

4. CHIME High-Priority Products (HPPs) and Selected Application Domains

HPPs, as mentioned above, are high-level mission deliverables derived from CHIME's core specifications and explicitly aligned with the Mission Requirements Document (MRD), to ensure strategic value for both scientific communities and downstream industry. Each HPP is tuned to CHIME's instrument specification (spectral bands, signal-to-noise ratio, spatial resolution). In this framework, HPPs are able to support the mission not only scientifically but also operationally, ready for integration in different Earth Observation downstream services [36,37].

4.1. Selected CHIME HPPs and Additional Products

4.1.1. Vegetation

Vegetation status assessment and monitoring require hyperspectral data to meet specific user requirements and to ensure accurate and meaningful analysis. These include the following:

- Spectral Requirements: High spectral resolution (≤10 nm) is essential to capture fine variations in spectral signatures, allowing differentiation of species-specific traits, detection of subtle stress signals, and analysis of biochemical and structural attributes [38];
- Spatial Requirements: High spatial resolution (≤20 m) is critical for mapping ecosystem heterogeneity, particularly in diverse or fragmented landscapes, enabling detailed monitoring of species distributions and habitat conditions [39];
- Temporal Requirements: Frequent temporal resolution, with revisit times of less than 10 days, is necessary to monitor phenological changes, track seasonal dynamics, and assess short-term responses to environmental stressors [40];
- Calibration and Validation: Accurate calibration, georeferencing, and access to field validation data are fundamental for ensuring that hyperspectral observations are reliable and comparable across time and space [41,42];
- Data Accessibility and Processing: Availability of user-friendly platforms and processing tools is vital to allow researchers and users to analyze data effectively, ensuring timely application of insights in biodiversity management and policymaking.

Orbiting satellite hyperspectral sensors, such as PRISMA and EnMAP, partially meet these requirements, enabling transformative advances on different scales [24]. Future satellite missions, such as CHIME, SBG and IRIDE, are developed to fully meet these technical requirements [7,43].

4.1.2. Raw Materials—Mineral Mapping

Hyperspectral imaging has become a revolutionary tool in mineral mapping, in particular due to its ability to detect diagnostic spectral features associated with specific minerals and geological processes and components [44]. The electromagnetic spectrum provides a powerful tool for understanding the characteristics of rocks and minerals through the interpretation of spectral features across different wavelength regions. Sensors like EMIT [45], PRISMA [46], and EnMAP [47] provide high-quality hyperspectral data in the VNIR-SWIR ranges, with improved spatial, spectral, and radiometric performance. EMIT, for example, is particularly suited for detecting surface mineral dust, offering insights into the mineralogical composition of arid and semi-arid regions. PRISMA and EnMAP provide broad applications for mineral alteration mapping and lithological boundary delineation with resolutions suitable for regional and site-specific investigations [48]. With spectral resolutions of around 10–20 nm and spatial resolutions between 20 and 30 m, these sensors are ideal for resolving fine mineral absorption features while capturing regional-scale geological variability [49]. High radiometric accuracy ensures reliable quantitative classifications of minerals, in terms of percentage in the pixel, even in complex terrains [50]. The integration of these advanced sensors into mineral exploration workflows has enabled detailed mapping of mineralogical processes, supported sustainable resource exploration, and improved environmental monitoring in mining regions [47,49,51].

4.1.3. Raw Materials—Methane Mapping

Gas detection is a critical application of hyperspectral imaging, especially for monitoring greenhouse gases (GHGs), such as methane (CH_4) and carbon dioxide (CO_2). This has garnered increased attention in recent times, in particular for climate change-related studies [52]. The SWIR range (1600–2500 nm) is particularly well suited for this purpose, as it encompasses the strong absorption features of these gases. These spectral features enable the identification of gas source points and proxy for the quantification of their concentration, considering the specific absorption feature in the SWIR region [53]. For instance, methane exhibits distinctive absorption bands at approximately 1660–1680 nm and 2300–2400 nm, making the SWIR range indispensable for plume detection, flux quantification, and monitoring multi-source emissions [22,54]. High spectral resolution, typically below 5 nm, is crucial for resolving these fine absorption features. Additionally, a high signal-to-noise ratio (SNR) is essential for capturing faint gas signatures, especially in areas with mixed or noisy backgrounds.

Spatial resolution of $\leq$50 m is required to pinpoint localized emission sources and effectively track plume dispersion patterns [55], which is critical for assessing industrial emissions, natural gas leaks, and other point sources [54]. Operational hyperspectral sensors, such as PRISMA and EMIT, have demonstrated exceptional capabilities in gas detection and monitoring. PRISMA, with its VNIR-SWIR coverage, has been successfully used to identify methane plumes, offering critical insights into emission dynamics [56]. EMIT, originally focused on mineral dust source mapping, has also shown potential for detecting greenhouse gases in specific applications [57]. These advancements are instrumental in air quality research and climate change mitigation, providing actionable data to reduce greenhouse gas emissions and address environmental challenges [58].

5. Materials and Methods

5.1. Review Design and Reporting

This work presents a systematic review of literature studies dealing with the retrieval of selected HPP products, such as vegetation-related variables and mineral and methane mapping. This review has been conducted using two scientific databases, Scopus and Web of Science (WOS). The algorithms applied in each study were evaluated, considering C/PB, ML, DL algorithms and hybrid models and comparing recent innovations and traditional approaches. This manuscript is aligned with the PRISMA checklist for systematic reviews (Figure 3). This systematic review was conducted by a single reviewer; thus, some PRISMA items were not fully met, specifically those related to duplicate screening and duplicate data extraction. All other steps of the review process adhered to PRISMA recommendations, using a standardized Excel form.

5.2. Data Sources and Search Strategy

The comparison between C/PB algorithms, ML algorithms and hybrid models was carried out following specific criteria, also with the aim to underline the specific role of hyperspectral data in the algorithm's development and application.

The systematic review was conducted following three main steps (Figure 4):

1. Application domains and product selection: Two application domains have been identified, vegetation and raw materials. Both application domains were selected in light of their central role in the CHIME mission framework and their relevance in the current European and international policy priorities, including ecosystem monitoring and Critical Raw Materials Act. For each application domain, the HPPs (marked by *) or additional products investigated are as follows:
    - Vegetation: Canopy Water Content (CWC)*, Vegetation Chlorophyll Content (CC)*;
    - Raw materials: mineral mapping (e.g., kaolinite)*, methane mapping.
2. Algorithms categorization: C/PB algorithms—ML/DL algorithms—hybrid models. Studies were classified as C/PB if variable retrieval was primarily driven by explicit physical models, even if ML is used as a secondary tool for the optimization of parameter or post-processing phase. Conversely, studies are categorized as ML-based when the target variable is directly evaluated through statistical learning retrieval. Finally, when physical models and ML are jointly explicitly integrated within the processing chain, the study is classified as hybrid.
3. Metrics of algorithm evaluation approach. This phase is deeply explained in the following sections. This organization categorizes the methods according to the specific

needs of hyperspectral data processing, providing a clear view of existing strategies. Then, a comparative analysis was carried out to highlight the main limitations of classical approaches and assess how ML/DL can address them in each application domain. To make this analysis clearer, comparative tables were constructed, integrating up-to-date scientific references.

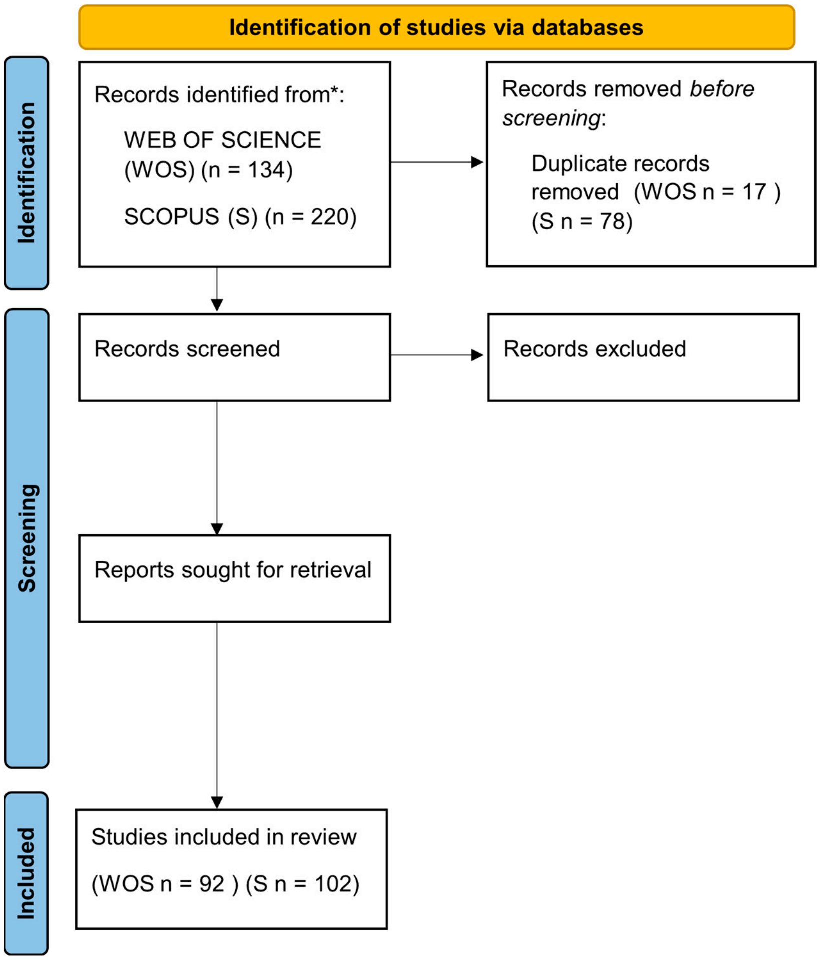

Figure 3. PRISMA 2020 flow diagram illustrating the systematic search and study selection process (Sections 5.1–5.5), including identification, screening, eligibility, and inclusion phases. The diagram reports the number of records retrieved from Scopus and Web of Science, duplicates removed, records screened, and studies included in the final synthesis. The asterisk (*) indicates that the reported number corresponds to the combined total of records retrieved from the two databases considered. Arrows represent the sequential progression of records through the review process. Colors are used solely to visually distinguish the different PRISMA phases.

5.3. Eligibility Criteria and Study Selection

The research strings customized for WoS and SCOPUS databases are reported as Supplementary Materials. A general visualization of used strings for each product is shown in Tables 4 and 5, related to C/PB algorithms and AI/ML/DL/hybrid models, respectively. No sensitivity analysis was conducted due to the heterogeneity of the methods. Eligibility studies included peer-reviewed articles published from 2015 to 2025 [24], written in English, which exploit hyperspectral remote sensing data for the analysis of the selected application domains [59]. The timeframe selected reflects key development period in hyperspectral sensors and algorithmic updates, including the transition toward new kinds of approaches where ML/DL and hybrid frameworks are involved. Duplicates and not strictly related studies were excluded. In addition, studies not reporting accuracy metrics were excluded in the eligibility screening stage of the papers considered.

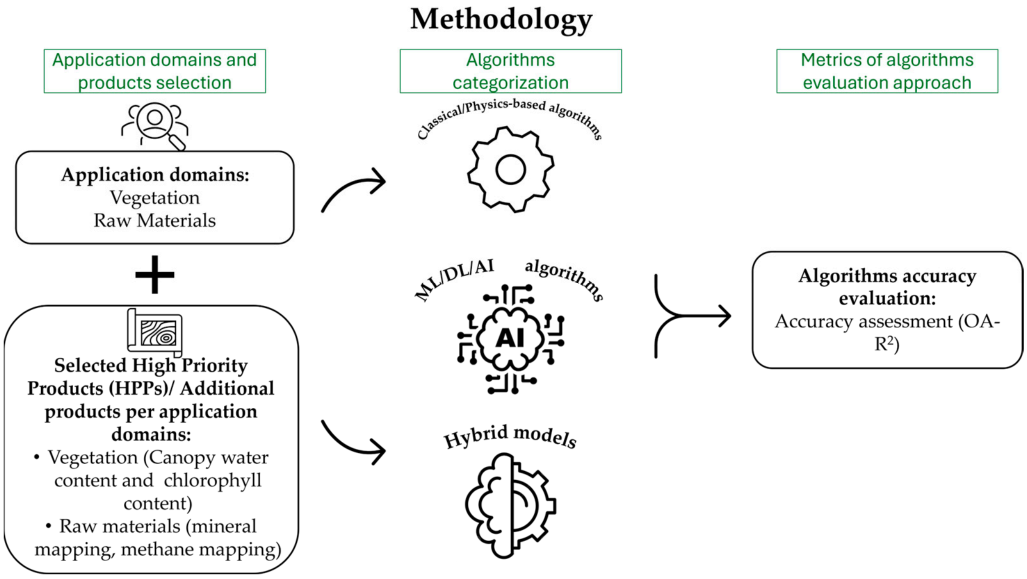

Figure 4. Methodology workflow of the review. The research followed a three-stage process: (1) two application domains were identified and the corresponding High-Priority Products were selected (**left**); (2) studies addressing the retrieval of these products were categorized according to the algorithm used (**center**); (3) the accuracy metrics reported in the studies were compared to evaluate which algorithm achieved the highest accuracy (**right**).

Table 4. Research strings for C/PB algorithms analysis.

Research String	Application Domain	HPP/Additional Product
Results for AB = ("hyperspectral data") AND AB = ("canopy water content") AND AB = ("algorithms")	Vegetation	Canopy Water Content (CWC)
Results for AB = ("hyperspectral data") AND AB = ("chlorophyll") AND AB = ("algorithms")	Vegetation	Chlorophyll Content (CC)
Results for AB = ("hyperspectral data") AND AB = ("mineral mapping") AND AB = ("algorithms")	Raw materials (mineral)	Mineral abundance mapping
Results for AB = ("hyperspectral data") AND ALL = (gas) AND AB = ("algorithms")	Raw materials (gas)	Methane mapping

It is important to underline that, despite the filtering process considering only hyperspectral data, to overcome the specific limitation of these data (i.e., low revisit time), several works used HSI in synergy with other optical sensors. This information has been collected and analyzed together with hyperspectral applications.

Table 5. Research key for AI/ML/DL and hybrid algorithms.

Research String (ML/AI/DL)	Application Domain	HPP/Additional Product
AB = ("hyperspectral data") AND AB = ("canopy water content") AND AB = ("algorithms") AND AB = ("machine learning" OR "artificial intelligence" OR "deep learning")	Vegetation	Canopy Water Content (CWC)
AB = ("hyperspectral data") AND AB = ("chlorophyll") AND AB = ("algorithms") AND AB = ("machine learning" OR "artificial intelligence" OR "deep learning")	Vegetation	Chlorophyll Content (CC)

Table 5. *Cont.*

Research String (ML/AI/DL)	Application Domain	HPP/Additional Product
AB = ("hyperspectral data") AND AB = ("mineral mapping") AND AB = ("algorithms") AND AB = ("machine learning" OR "artificial intelligence" OR "deep learning")	Raw materials (mineral)	Mineral abundance mapping
AB = ("hyperspectral data") AND ALL = (methane) AND AB = ("algorithms") AND AB = ("machine learning" OR "artificial intelligence" OR "deep learning") AND ALL = (gas) AND AB = ("algorithms")	Raw materials (gas)	Methane mapping

5.4. Risk-of-Bias Assessment

To evaluate the methodological robustness across the studies included in the research, a specific risk-of-bias (RoB) tool was developed. Standard risk-of-bias instruments, such as QUADAS-2, ROBINS-I, PROBAST, Cochrane RoB, were not used because they were designed for clinical trials, diagnostic accuracy studies, or predictive models with human subjects. These are not designed for algorithm development studies in hyperspectral remote sensing, where biases arise mainly from the dataset construction, validation and metric reporting.

Starting with this assumption, a tailored PRISMA-aligned approach was conducted to assess the risk of bias. Four characteristics were considered: (C1) dataset quality and representativeness, (C2) validation design and overfitting control, (C3) accuracy and reporting, (C4) transparency and reproducibility. These characteristics were used to rate each work as low, high or unclear RoB, according to the explicit analysis criteria better explained in Table 6.

Table 6. Risk-of-bias analysis criteria categories.

Category	Low Risk	High Risk	Unclear
C1—Dataset quality	Adequate sample size; multi-scene or multi-site dataset; clear ground truth	Very small or single-scene dataset; poorly defined ground truth	Insufficient dataset description
C2—Validation design	Independent test set and/or well-defined CV	No clear train/test separation; ambiguous validation	Validation referenced but not described
C3—Accuracy reporting	Complete metrics (e.g., R^2 + RMSE; OA + F1) with uncertainty estimates	Incomplete or inappropriate metrics; no uncertainty; training-only results	Metrics reported without context or clarity
C4—Transparency and reproducibility	Clear description of methods, preprocessing, parameters; code available	Major methodological details missing	Partial information

For each study, a value was assigned to each characteristic (C1–C4): 0 (satisfied), 1 (not satisfied). If the overall value was higher than 1, the RoB for the selected paper was rated as high; if the risk was low within the four-category system, the final classification of bias was low; and if some of the criteria were not satisfied or not specified in the work analyzed, the paper was rated as unclear. The distribution of high-risk ratings (C1 and C2) showed very few high-risk cases but a high proportion of unclear ratings due to insufficient reporting. C3 (accuracy reporting) exhibited the largest concentration of high-risk ratings, with approximately 55% of vegetation and methane studies and approximately 40% of mineral studies failing to report complete or standardized metrics. C4 (transparency) showed almost no high-risk ratings but widespread unclear assessments, especially in machine learning (ML)/deep learning (DL) papers, where preprocessing and hyperparameters were often underreported. Overall, insufficient reporting, rather than poor methodological design, was the primary contributor to RoB in hyperspectral studies.

5.5. Performance Metrics and Comparative Analysis

In order to compare the different algorithm categories, the following accuracy metrics were considered: (1) coefficient of determination (R^2), mainly for regression-based studies (e.g., methane, CWC), and (2) Overall Accuracy (OA). The R^2 quantifies how well the model's predictions reproduce the variability in the value of a reference variable. Higher R^2 values indicate that the algorithm captures a larger proportion of the true spectral–biophysical variability. The OA expresses the proportion of correctly classified samples over the total number of validation samples. It is the standard metric for mineral mapping, where outputs are categorical classes (e.g., kaolinite), and continuous regression metrics such as R^2 are not applicable. These two metrics were selected because they were used in all the papers analyzed and reported most consistently across the scientific literature, facilitating the comparison among heterogeneous algorithm categories These enable a more in-depth explanation of two dominant retrieval problem types in hyperspectral data analysis: regression and classification. Due to the heterogeneity in sensors, datasets, and validation strategies, a descriptive comparative analysis was performed instead of a meta-analysis. To capture performance variability, highlight methodological trends, and identify differences between C/PB, ML/DL, and hybrid approaches, the minimum and maximum R^2 or OA values were extracted for each product and algorithm category. When relevant, the use of hyperspectral multi-sensor synergies was also noted, particularly in methane and mineral mapping applications.

6. Results

The Results Section provides a synthesis of the reviewed studies, organized by application domain, target product, algorithm category, sensor platform and covered spectral ranges. Considering the large number and heterogeneity of the included studies, their specific key characteristics, such as data source (UAV, airborne, multi-sensor, etc.), methodology and the primary research objective, are reported in an aggregated and comparative form instead of an individual study summary. This approach enables the identification of robust methodological and sensor ware trends across the selected literature. In particular, in this systematic review, a total of 194 scientific papers were analyzed across the two considered application domains (i.e., vegetation and raw materials), after a first phase of screening to remove duplicates and studies which did not report accuracy metrics. The literature was collected from two leading scientific databases: Web of Science, (WoS) with 92 papers, and Scopus, contributing 102 papers (Figure 4). An overview of the data extraction template, listing the column names extracted during the screening phase, is provided in the Supplementary Material (Table S1).

Figure 5a shows a summary of the number of scientific papers analyzed, dividing them by application domain and product. More papers were related to chlorophyll content retrieval in the vegetation application domain (107), followed by methane mapping (55) and mineral mapping (23) for the raw materials domain. Finally, the canopy water content in the vegetation domain is the least studied, with only nine papers. Figure 5b shows the growing use of hyperspectral data over the time period considered in this review divided by application domain and product.

The tailored risk-of-bias (RoB) assessment revealed that many studies were limited by incomplete reporting. This analysis suggested that the main limitation lies in the under-reporting of methodological details.

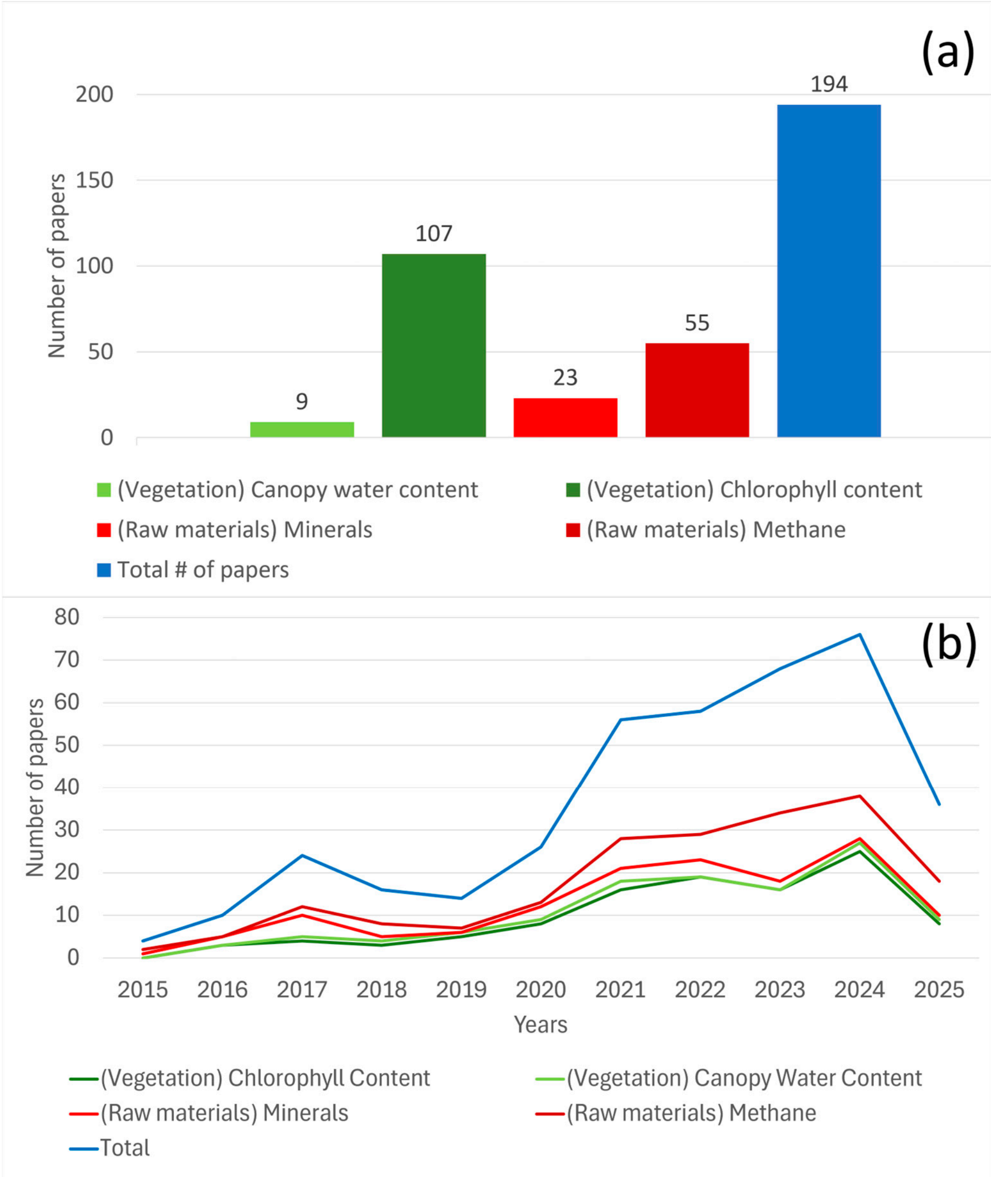

Figure 5. Number of papers analyzed in this systematic review: (**a**). Total number of papers analyzed for each application domain and product; (**b**) timeline of published papers for each application domain and product. The negative trend in 2025 is representative only of the first part of the year (until July 2025).

Considering the large number and the heterogeneity of the reviewed studies, the main characteristics, such as primary research objective, dominant algorithmic approach and data source, are summarized in Table 7.

The first result extracted from the review is related to the most relevant spectral ranges used for each application domain considered. This result allow us to more accurately detail the information compared to Table 1. This confirmed that the VNIR-SWIR range (400–2500 nm) is the core spectral domain for the retrieval of vegetation properties and mineral mapping, with almost 88%, 56% and 91% of the studies using this range for chlorophyll, CWC and mineral retrieval, respectively. The SWIR range (900–2500 nm) is particularly used for mapping methane.

For methane and mineral mapping, thermal IR (7500–13500 nm) is also used, while MWIR (3000–5000 nm) has limited importance for these application domains (Figure 6).

Table 7. Aggregated overview of the main characteristics of the reviewed studies across application domains and products.

Application Domain	Product	Primary Research Objective	Dominant Algorithm Category	Main Data Source
Vegetation	CWC	Quantitative biophysical retrieval	ML/Hybrid	Field, UAV
Vegetation	CC	Quantitative biophysical retrieval	ML/DL	Field, UAV, Satellite
Raw materials	Mineral mapping	Detection/abundance mapping	C/PB	Airborne, Satellite
Raw materials	Methane mapping	Detection and mapping	C/PB/Hybrid	Airborne, Satellite

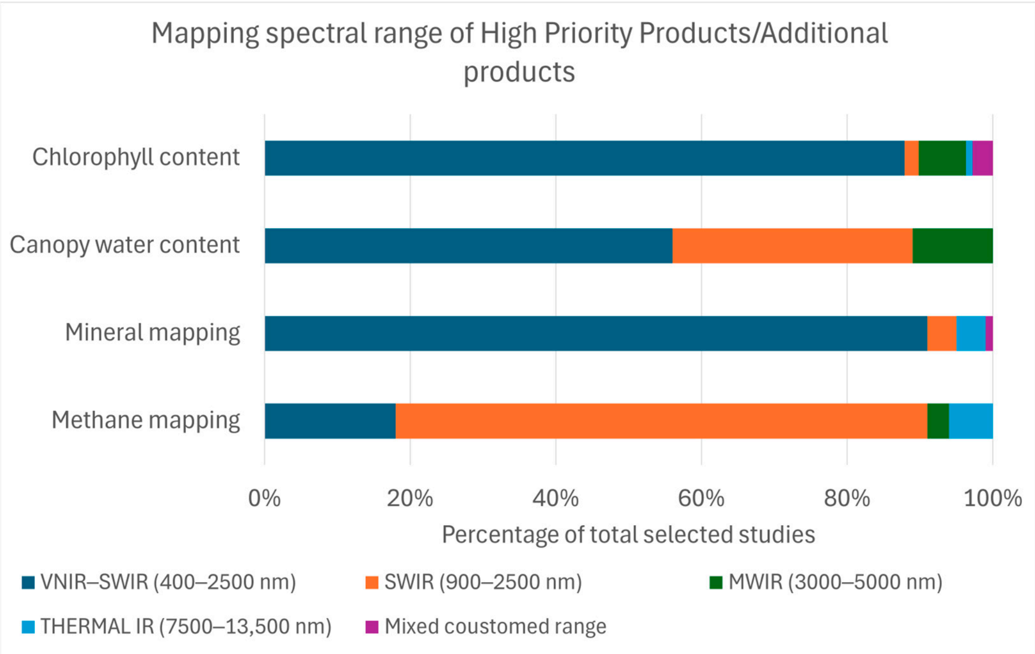

Figure 6. Percentage of papers that used specific electromagnetic spectrum ranges for the retrieval of the products.

6.1. Vegetation

The following paragraphs will repots the findings of this review for the vegetation domain, divided by canopy water content and chlorophill content. Four results will be reported for each product: (1) the most commonly used algorithm, (2) the most common sensor platform, (3) the most used spectral ranges, and (4) the accuracy metric values.

6.1.1. Canopy Water Content (CWC)

The evaluation of a parameter like the canopy water content (CWC) has undergone a notable evolution from C/PB models to modern algorithms (ML or hybrid approach). The most used algorithm for this parameter is ML, which accounts for 56% of the total methodologies applied for CWC evaluation (Figure 7). On the other hand, C/PB approaches, for example, Radiative Transfer Models (RTMs) and empirical relationships, represent 22% of the total. Hybrid approaches that combine physical modelling with ML account for 11%, as well as deep learning (DL). Specifically, the algorithms used are as follows (Figure 7):

- The C/PB partial least squares regression (PLSR) and its relative hybrid combination with the artificial neural network (PLSR-ANN hybrids) account for 23%, emphasizing the traditional stronghold of linear latent space techniques adapted to hyperspectral complexities.

- We found that 18% of the studies investigated show that ML algorithms, such as Boosting and tree-based ensemble methods (e.g., Random Forest, XGBoost, CatBoost, LightGBM, Extremely Randomized Trees), are among the most popular. Their ability to capture non-linearities and handle high-dimensional data makes them particularly suited to hyperspectral analysis.
- The ML Gaussian Process Regression (GPR) represents 18%, although powerful for uncertainty estimation, likely due to its computational cost on large hyperspectral datasets.
- The ML Support Vector Machines (SVM/SVR) account for 12%, typically preferred for their robust generalization in medium-sized datasets.
- CNNs, autoencoders and MDN variants, which are DL models, represent only 6%.
- C/PB approaches, bundled under "other" (RTMs, LUTs, empirical relations), retain a significant niche on this domain (23%).

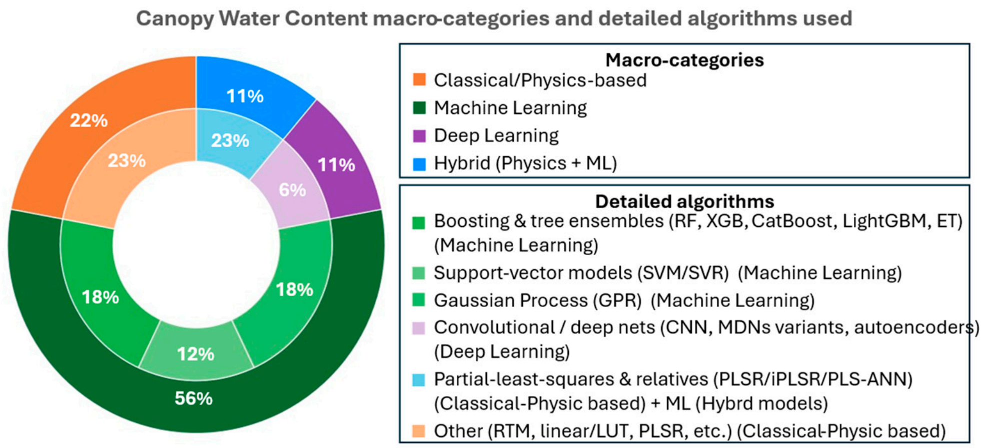

Figure 7. Most used algorithms for canopy water content retrieval: the outer circle represents the categories of algorithms (i.e., C/PB, ML, DL or hybrid models); the inner circle represents, in each category, the most used algorithms.

The following sensor platforms were used to assess CWC (Figure 8):

- Field spectroradiometers are the most commonly used instrument in studies (31%), confirming that field-calibrated data remain the gold standard for model development and validation.
- Spaceborne and airborne hyperspectral systems, such as PRISMA, AVIRIS-NG, and EnMap (15%), are now significant contributors, reflecting the maturation of satellite hyperspectral missions.
- UAV-mounted hyperspectral sensors and airborne systems each contribute 8 and 23%, respectively, indicating the rising relevance of flexible, high-resolution platforms for local and regional studies.
- The multispectral spaceborne Sentinel-2 MSI system also appears with 8%, despite its spectral limitations for precise water absorption feature detection.

These results emphasize the importance of spectral representation fidelity (hyperspectral spectroradiometer) and spatial flexibility (UAVs) in current CWC research.

Finally, the spectral ranges utilized in CWC retrieval (Figure 9) point to a preference for broad, high-information content ranges:

- Full-range VNIR-SWIR coverage (400–2500 nm) is the most exploited (~55%), confirming that key water absorption features at 970 nm, 1200 nm, 1450 nm, and 1940 nm are critical for accurate estimation.

- VNIR-only sensors (400–1000 nm) are used in about 30% of cases, primarily when SWIR coverage is unavailable due to radiometric limitations (e.g., high noise level).
- SWIR-only windows (e.g., 2100–2300 nm) and thermal infrared (TIR, 7000–12,000 nm) are minimally used, indicating that, despite being useful for stress detection, they are less informative for direct water quantification.

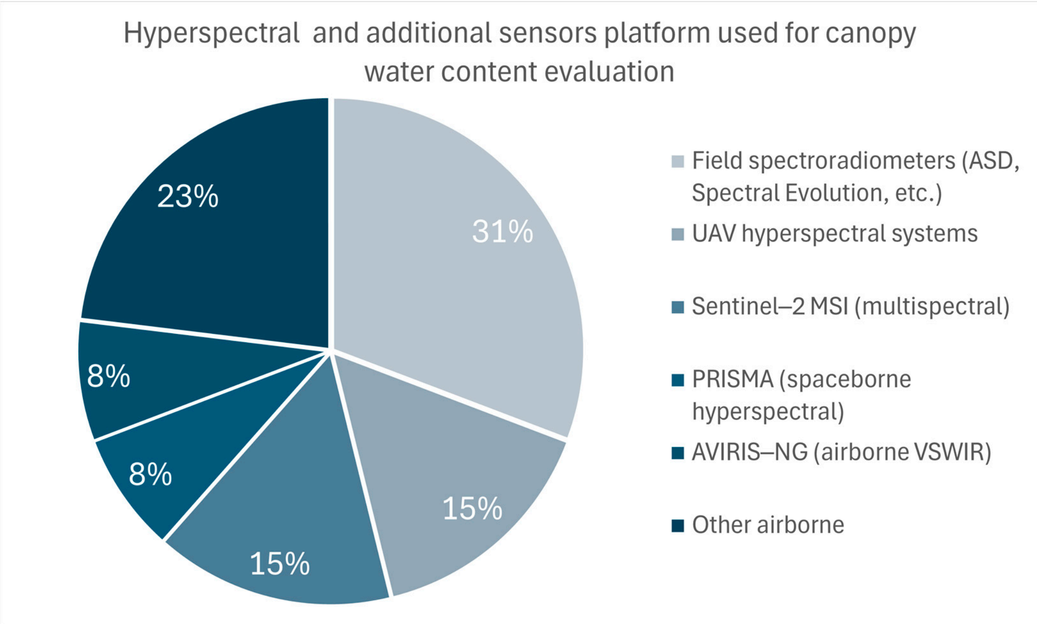

Figure 8. Hyperspectral and additional sensor platforms used for canopy water content retrieval.

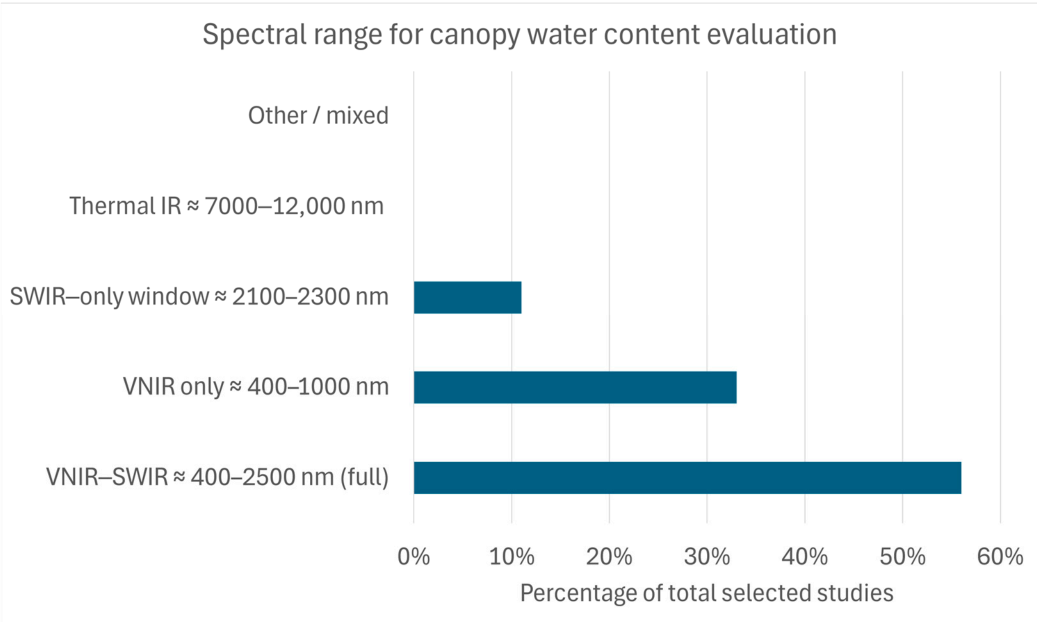

Figure 9. Spectral ranges used for the estimation of canopy water content.

This result emphasizes the importance of accessing both the VNIR and SWIR domains to fully capture the spectral signatures related to CWC.

Finally, a comparison of algorithm performance is shown in Figure 10. The accuracy metrics (R^2) indicated in the studies are the following:

- Machine learning approaches exhibit the widest R^2 range, from a minimum of 0.58 to a maximum of 0.95, suggesting high variability but also remarkable potential for excellent predictions under optimal conditions.
- For hybrid models (ML + RTM), just one paper was analyzed, presenting an R^2 value of 0.78.
- Physics-based methods show the narrowest and generally lower R^2 values (0.448–0.665), highlighting the limitations of purely physical models when confronted with complex canopy heterogeneity and non-linear water content responses.

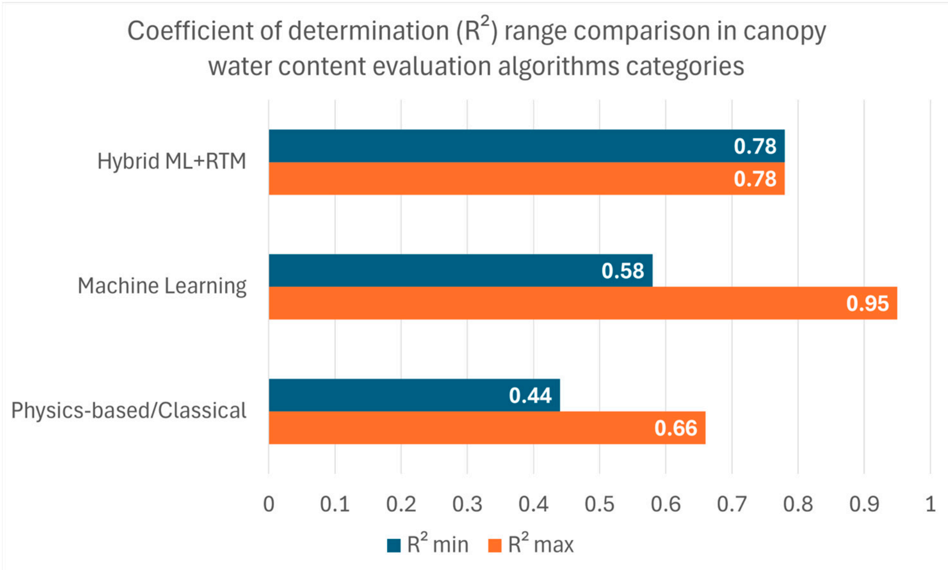

Figure 10. Coefficient of determination (R^2) range comparison in canopy water content evaluation algorithm categories. The blue bars indicate the minimum value of R^2 reported, while the orange bars indicate the maximum value.

The wide R^2 range observed for physics-based approaches reflects the heterogeneity of physical modelling strategies collected in this work (from empirical regression to RTM inversion) and experimental conditions across studies, rather than inconsistent performance of some methods themselves.

6.1.2. Chlorophyll Content (CC)

The application of ML algorithms dominates studies on CC, being employed in 59% of the reviewed studies (Figure 11). C/PB approaches, such as radiometric indices (e.g., NDVI variants, chlorophyll absorption ratios) and RTM inversions, account for 21%. Deep learning methods are employed in 12% of the analyzed studies, a slightly higher proportion than in CWC studies. Hybrid approaches (C/PB + ML) are emerging for the assessment of chlorophyll content (8%).

A breakdown of algorithmic families (Figure 11) reveals a clear preference structure:

- ML algorithms, such as Boosting and ensemble trees (Random Forest, XGBoost, CatBoost, LightGBM, Completely Random Forests), represent the most widely used group (28%), leveraging their capability to handle high-dimensional, noisy hyperspectral inputs.
- The C/PB PLSR (but also iPLSR) and its hybrid derivatives (PLS-ANN) retain a relevant role (21%).
- The ML Support Vector Machines (SVM/SVR), including semi-supervised extensions, account for 15%, typically used for cases with limited ground-truth data.

- Spectral–spatial DL architectures (CNNs, Mixture Density Networks, Deep Belief Networks) follow at 12%, indicating growing confidence in their capacity to model complex chlorophyll spectral signatures and spatial heterogeneity.
- The ML Gaussian Processes (GPRs), both homoscedastic and heteroscedastic, remain marginal (9%), again likely due to computational constraints for large datasets.
- C/PB models, including rule-based regression models such as Cubist, Multivariate Adaptive Regression Splines (MARS), logistic models, and direct Look-Up Table and Radiative Transfer Models (LUT/RTM) inversions, account for 8%, indicating that purely physics-based strategies are increasingly complemented by statistical corrections or optimizations.
- Finally, 7% of the algorithms considered are hybrid, in particular RTM combined with DL techniques, such as CNNs, or ML techniques, such as SVM.

Sensor platform analysis (Figure 12) shows, as well as for CWC, a marked preference for field-based measurements:

- Field spectroradiometers (e.g., ASD, PSR, SVC, Ocean Optics) dominate at 35%, confirming that field-level high-resolution data remain essential for calibrating and validating chlorophyll models.
- UAV-based hyperspectral platforms (Headwall, Cubert, GaiaSky, Pika) contribute a significant 25%, reflecting the requirement of high-spatial-resolution measurements at the canopy scale.
- Other platforms, including Sentinel-2 MSI, HyMap, DESIS, Hyperion, LiDAR-HS, and various CubeSat/MS solutions, represent 27%.
- Satellite and airborne sensors, such as PRISMA and AVIRIS-NG, appear at 7% and 6%, respectively.

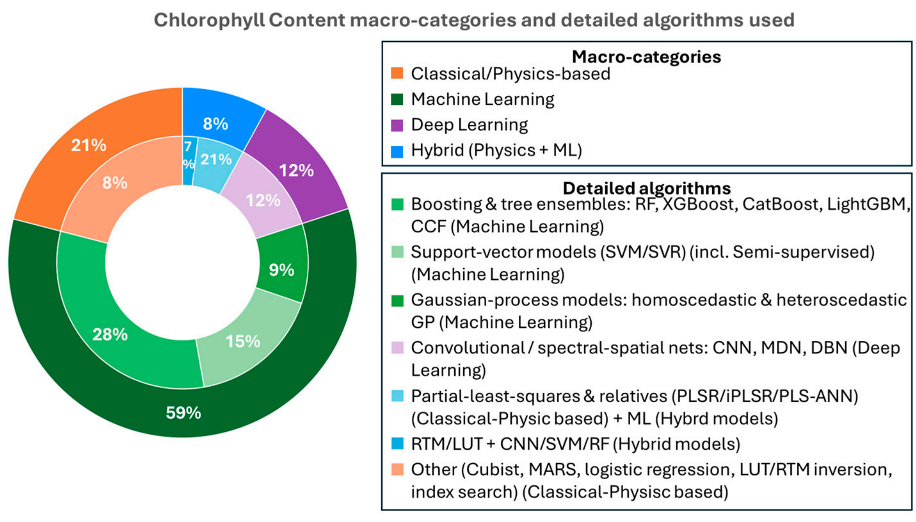

Figure 11. Most used algorithms for chlorophyll content estimation: the outer circle represents the categories of algorithms (i.e., C/PB, ML, DL or hybrid models); the inner circle represents, in each category, the most used algorithms.

It is evident from Figure 13 that the full VNIR-SWIR range (400–2500 nm) is employed in the majority (more than 85%) of studies for CC estimation. This full spectral range is crucial for capturing the multiple absorption features related to chlorophyll, as well as for the CWC.

VNIR-only (400–1000 nm) approaches are rare (~5–8%), and the utilization of SWIR-only, MWIR, or TIR ranges is low or negligible, underscoring the necessity of broad spectral coverage to accurately isolate chlorophyll signals from background variability.

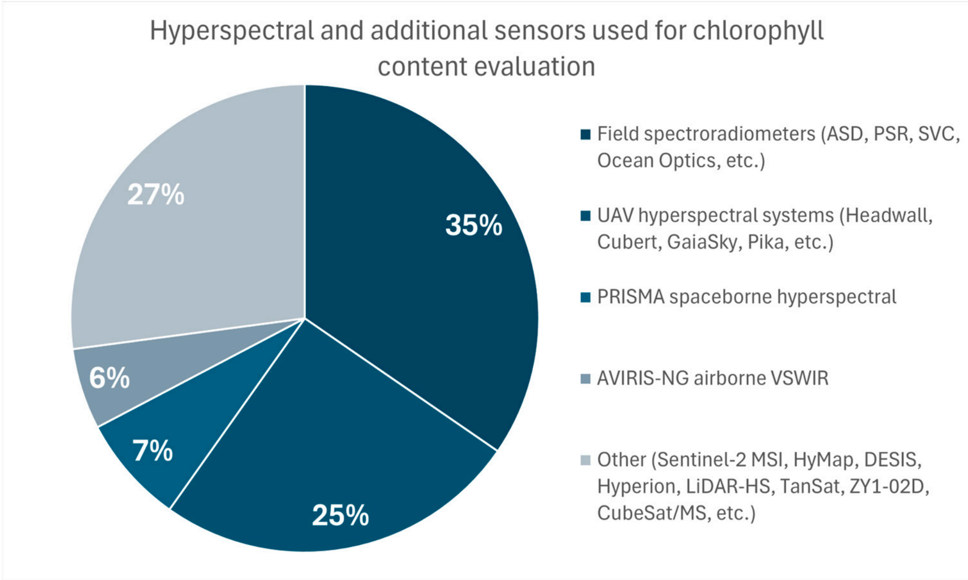

Figure 12. Hyperspectral and additional sensor platforms used for chlorophyll content estimation.

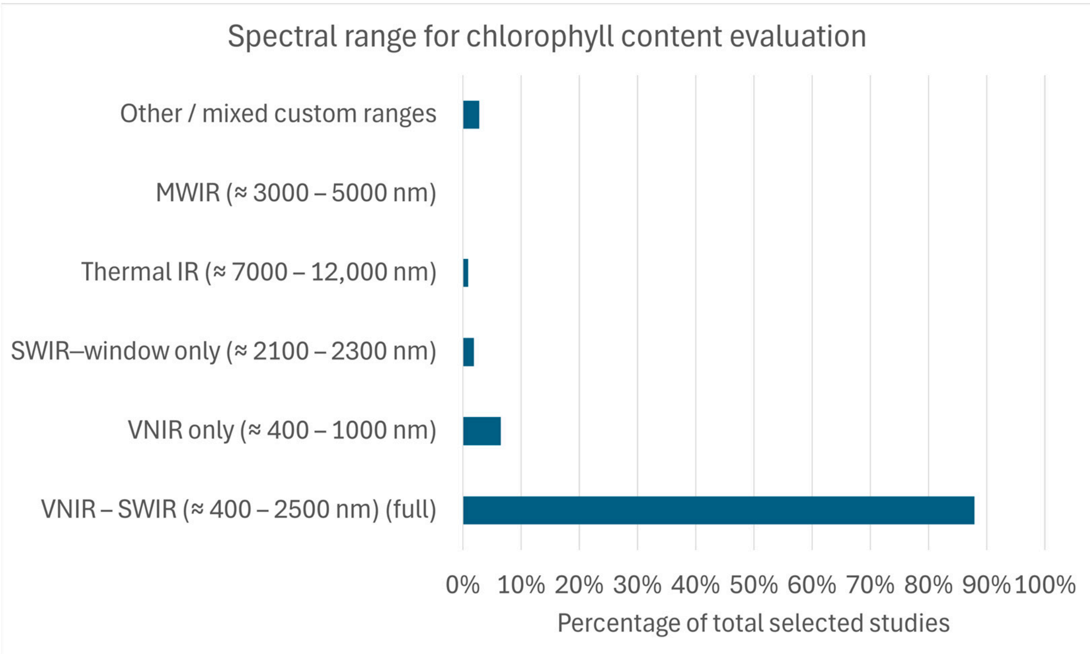

Figure 13. Spectral ranges used for the estimation of chlorophyll content.

The performance analysis based on the coefficient of determination (R^2) (Figure 14) reveals important trends:

- DL models follow closely, with R^2 ranging from ~0.8 to ~0.98, reflecting their ability to model complex non-linear spectral signatures, albeit with higher sensitivity to training data quality.
- Pure ML models show greater variability, with R^2 from ~0.44 to ~0.99, emphasizing that, without physical constraints, the models can perform extremely well but also risk underfitting or overfitting in heterogeneous conditions, according to the analyzed papers.

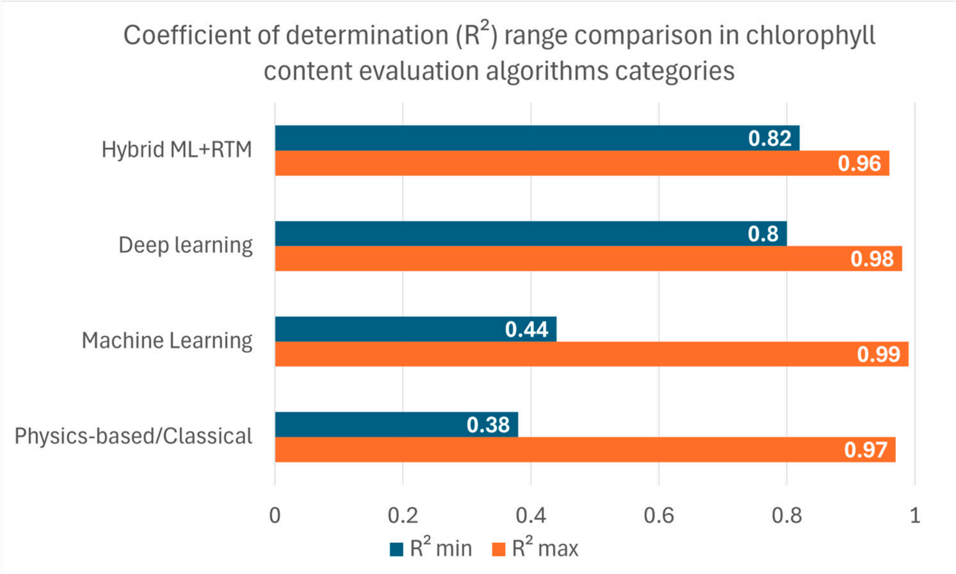

Figure 14. Coefficient of determination (R^2) range comparison in chlorophyll content evaluation algorithm categories. The blue bars indicate the minimum value of R^2 reported, while the orange bars indicate the maximum value.

6.2. Raw Materials

The following paragraphs report the findings of the reviews for the raw materials domain, divided by mineral mapping and methane mapping. Four results will be reported for each product: (1) the most commonly used algorithm, (2) the most common sensor platform, (3) the most used spectral ranges, and (4) the accuracy metric values.

6.2.1. Mineral Mapping

A detailed analysis of the studies reviewed provides key insights into algorithm usage, sensor deployment, spectral preferences, and performance metrics.

In contrast to vegetation applications, C/PB methods dominate mineral mapping studies, comprising 52% of the algorithms analyzed (Figure 15). These include techniques such as Spectral Angle Mapper (SAM), Matched Filtering (MF), Linear Spectral Unmixing (LSU), and direct reflectance-based detection.

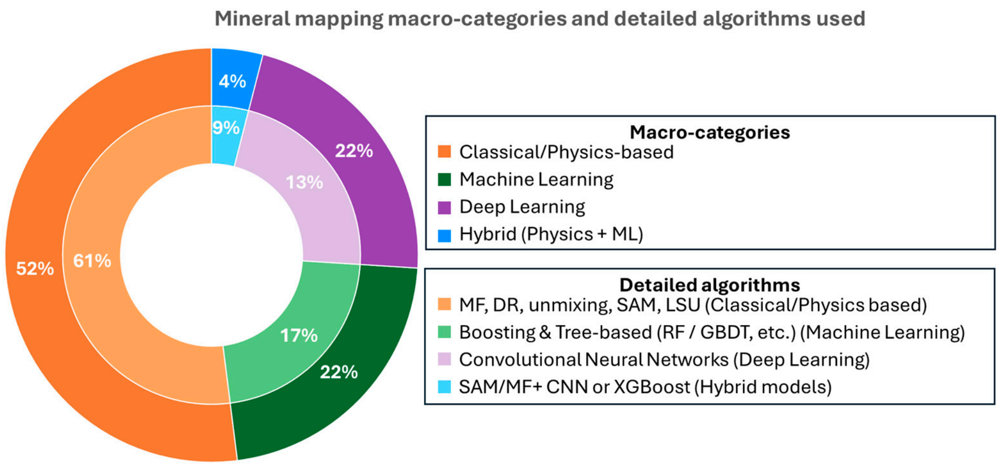

Figure 15. Most used algorithms for mineral mapping: the outer circle represents the categories of algorithms (i.e., C/PB, ML, DL or hybrid models); the inner circle represents, in each category, the most used algorithms.

Machine learning methods account for 22%, the same as deep learning methods (22%), while hybrid models (C/PB + ML) are still marginal (4%).

Analyzing the specific algorithm families (Figure 15), we find a clear traditional dominance:

- Classical/physics-based methods (SAM, LSU, MF) still dominate with 61% usage. These approaches exploit the well-defined spectral absorption characteristics of minerals, leveraging physics-based matching rather than data-driven pattern recognition.
- Boosting and tree-based ML algorithms (e.g., Random Forest, Gradient-Boosted Decision Trees) represent 17%, valued for their ability to discriminate subtle spectral mixtures and handle noisy field or airborne data.
- DL methods, such as Convolutional Neural Networks (CNNs), have started to gain traction (13%), particularly in high-complexity mapping scenarios, considering the analyzed references.
- Hybrid models are marginal (9%), mainly related to SAM/MF techniques added to an ML framework, for computation empowerment.

The analysis on the sensor and platform usage (Figure 16) highlights the dominance of airborne platforms:

- Airborne or satellite hyperspectral sensors (HyMap, DESIS, Hyperion, M3, ASTER, etc.) account for the majority (61%), reflecting the historical and ongoing importance of airborne hyperspectral mapping missions in mineral exploration.
- AVIRIS-NG, a high-performance airborne imaging spectrometer, is utilized in 13% of the studies, highlighting its high spectral resolution in the VNIR-SWIR.
- PRISMA (spaceborne hyperspectral) accounts for 17%, indicating the importance of hyperspectral satellite missions in large-scale mineral mapping.
- Thermal and longwave systems (e.g., HyTES, HySpex LWIR) are also represented (9%), important for detecting minerals with strong TIR emissivity features (e.g., carbonates, sulfates).

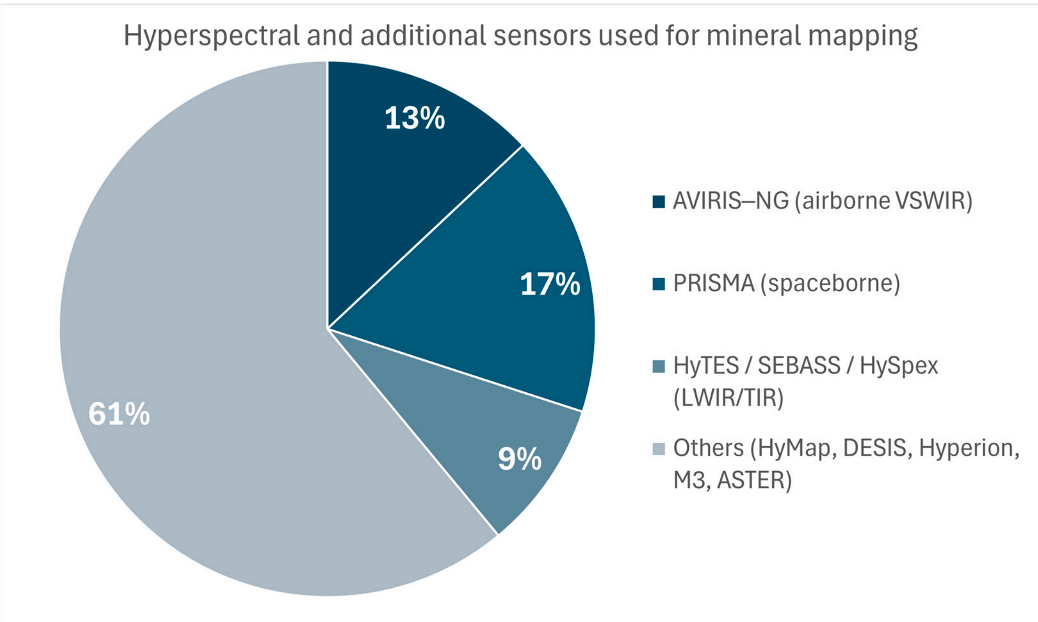

Figure 16. Hyperspectral and additional sensor platforms used for mineral mapping.

Most mineral mapping studies employ the full VNIR-SWIR range (400–2500 nm) (Figure 17), critical for capturing key mineral absorption features. Each mineral shows a different response in the electromagnetic spectrum:

- Al-rich phyllosilicates (Al-OH), such as Kaolinite, Illite, Muscovite, Pyrophyllite; iron-bearing phyllosilicates (Fe-OH), such as Nontronite, Ferruginous smectite, Goethite; magnesium-rich phyllosilicates (Mg-OH), for example, Talc, Chlorite, Saponite, Serpentine, which all have spectral features in the 2000–2500 nm SWIR region.
- Iron oxide features are pronounced in the 400 nm–1000 nm VNIR range.
- Some studies incorporate thermal infrared (TIR, 7000–12,000 nm) or MWIR (3000–5000 nm) data, but these remain minority cases (<5%), primarily used for advanced mineral classes (e.g., carbonates, sulfates).

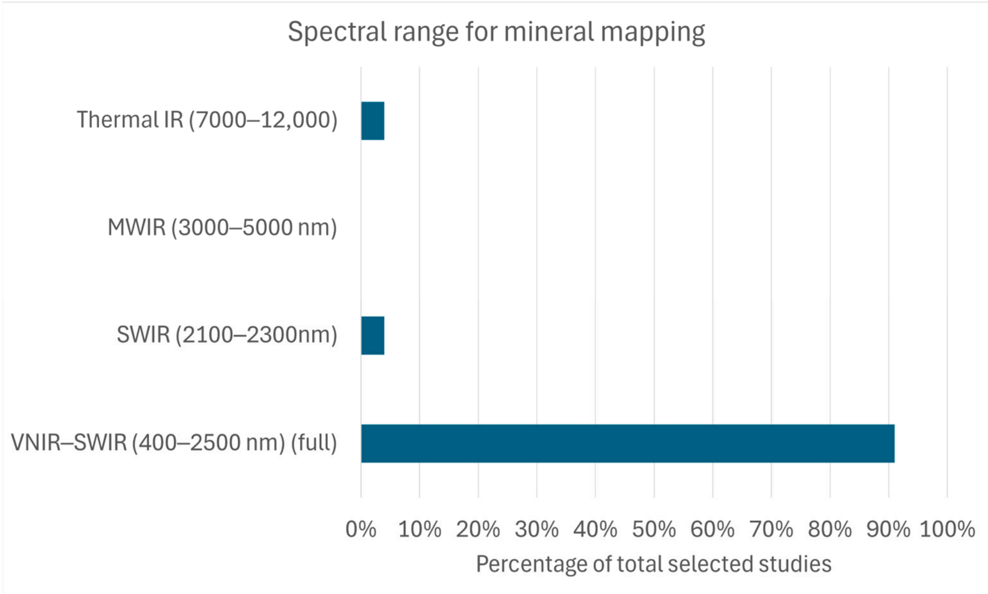

Figure 17. Spectral range used for mineral mapping.

The almost universal reliance on VNIR-SWIR confirms the fundamental importance of broad spectral coverage for accurate and discriminative mineral detection.

For this application domain, Overall Accuracy (OA) was selected as the primary comparative metric, because it was the most reported parameter across the reviewed references. Moreover, the R^2 parameter is not always applicable or reported, especially in classification tasks, such as mineral mapping. Overall Accuracy offers a standardized and interpretable measure of performance across classical, machine learning, and hybrid approaches. The comparison of Overall Accuracy (OA) across algorithm categories (Figure 18) reveals distinct performance characteristics:

- Deep learning models achieve high OA values, often ranging from 82.7% to 94.8%, reflecting their superior ability to model complex non-linear and spectral–spatial patterns, particularly in challenging or mixed-mineral scenes.
- Machine learning approaches show broader variability, with OA values from ~50% to ~90%, depending heavily on feature selection, training sample quality, and model tuning.
- C/PB methods, while highly interpretable and consistent, typically achieve slightly lower OA (ranging from ~54% to 80%), constrained by their inability to model subtle spectral variations and mixed pixel effects without manual intervention.
- Hybrid models achieve the highest OA values (80% to 96%).

While classical methods remain operationally dominant, the highest accuracies are increasingly obtained through hybrid models, especially in complex or high-resolution datasets.

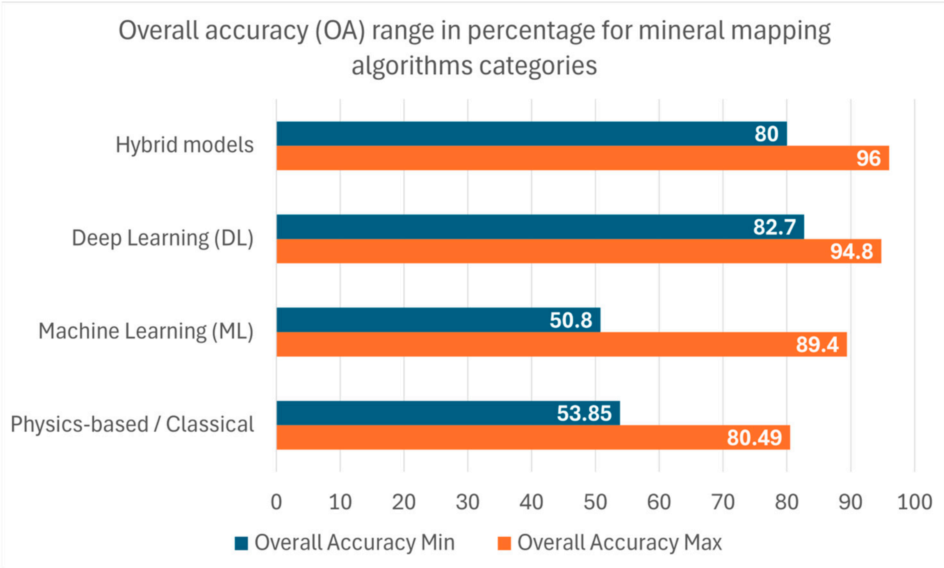

Figure 18. Overall Accuracy (OA) range in percentage for mineral mapping algorithm categories. The blue bars indicate the minimum value of R2 reported, while the orange bars indicate the maximum value.

6.2.2. Methane Mapping

The detection and quantification of methane (CH_4) by means of hyperspectral data are technically challenging, due to the weak and narrow spectral characteristics of methane compared with signals from vegetation and minerals. This literature review revealed critical patterns in the evolution of algorithmic approaches, sensor use, spectral range utilization and model performance.

Methane mapping remains heavily grounded in C/PB methods, which account for 64% of the reviewed studies (Figure 19). These methods include variants of Matched Filter (MF), Optimal Estimation, and Differential Optical Absorption Spectroscopy (DOAS). Machine learning methods are applied in 11% of the studies, while deep learning is slightly more prominent at 16%. Hybrid approaches (C/PB + ML) are still emerging, representing 9% of the cases.

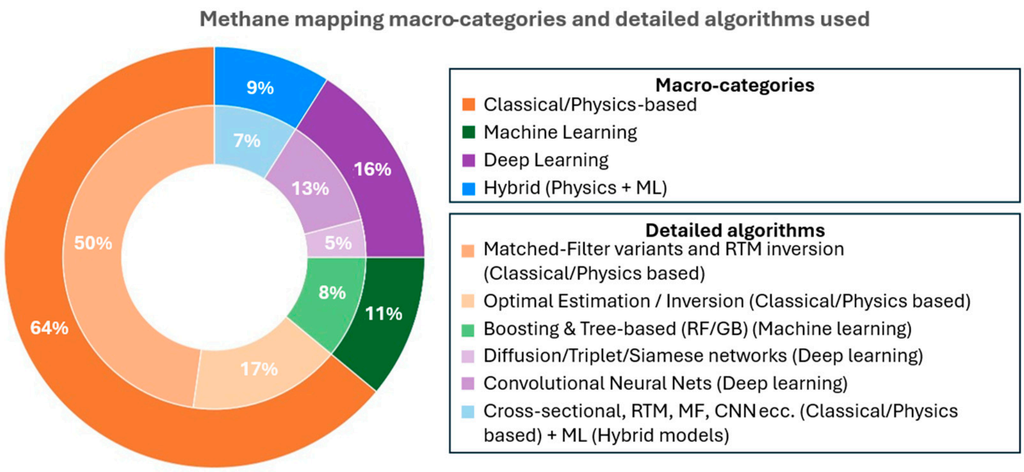

Figure 19. Methane mapping's most used algorithms: the outer circle represents the categories of algorithms (i.e., C/PB, ML, DL or hybrid models); the inner circle represents, in each category, the most used algorithms.

A breakdown of specific algorithm types (Figure 19) shows the following:

- As C/PB-based methods, Matched Filter variants (e.g., standard MF, Adaptive Matched Filter, AMF, Orthogonal Subspace Projection) dominate with 50%, exploiting known methane absorption features centered around ~2300 nm in the SWIR domain.
- Optimal estimation and inversion methods (17%) also play a central role, particularly in PB retrievals from spaceborne sounders, which is a specialized remote sensing instrument that measures the atmospheric temperature and moisture profiles by analyzing infrared (IR) radiation [60].
- DOAS and cross-sectional techniques (7%) are mostly used with hyperspectral sounders for column concentration retrievals but are included in Matched Filtering, associated with machine learning techniques such as the MLP (Multi-Layer Perceptron) as an innovative hybrid approach.
- Among machine learning-based approaches, Boosting/tree ensembles (8%) are the main techniques used for mineral mapping.
- Deep learning architectures, including diffusion models, triplet networks, Siamese nets (5%), and CNNs (13%), emerge as powerful tools to model the complex spatial structures of methane plumes and improve false-positive rejection.

Sensor platform analysis (Figure 20) highlights the diversity of methane sensing:

- AVIRIS-NG leads (31%), confirming its critical role in airborne, high-resolution methane mapping campaigns.
- PRISMA contributes to 15% of the studies, reflecting its promising capabilities for methane detection using spaceborne sensors.
- Other types of sensors, such as Sentinel-5P TROPOMI (13%), provide low-resolution methane presence products.
- EMIT (9%, ISS onboard) provides coarse resolution but large-scale methane monitoring.
- Thermal and LWIR sensors (HyTES, SEBASS, HySpex-TIR) account for 11%, critical for surface temperature corrections and, in some cases, direct methane thermal emission retrieval.
- Hyperspectral sounders (CrIS, IASI, AIRS) (7%) and other custom platforms (UAV-based, sUAS, custom TDLAS systems) together represent the remaining 14%.

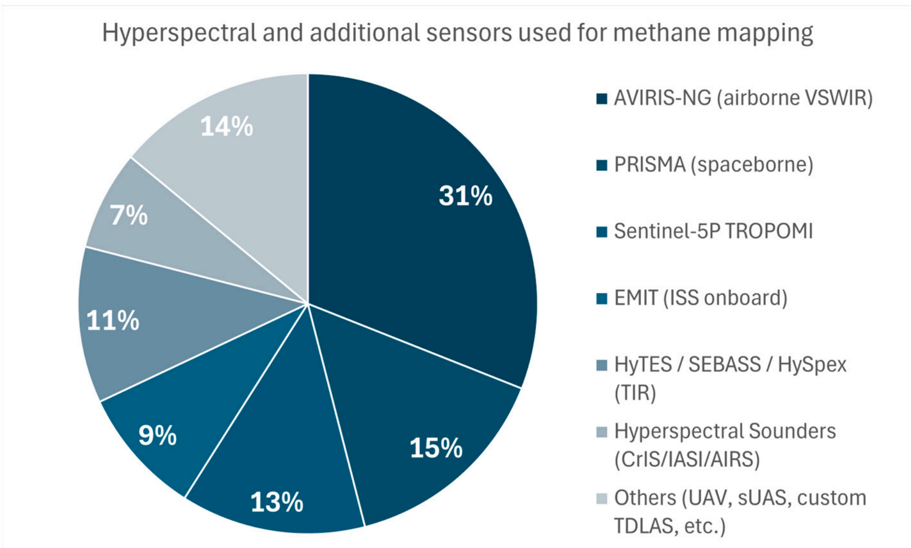

Figure 20. Hyperspectral and additional sensor platforms used for methane mapping.

Methane mapping relies overwhelmingly on the SWIR window (2000–2500 nm), as shown in Figure 21:

- Around 73% of the studies exclusively utilize the SWIR range, exploiting strong methane absorption features at ~2290–2310 nm.
- VNIR-SWIR full coverage is employed in ~20% of cases, mostly when multi-target mapping is considered (e.g., simultaneous vegetation or mineral studies).
- Use of MWIR (3000–5000 nm) (<5%) or TIR (7500–13,500 nm) (6%) remains marginal due to atmospheric absorption and weaker surface reflectance in these ranges for methane but of course related to the available hyperspectral sensor spectral range capability.

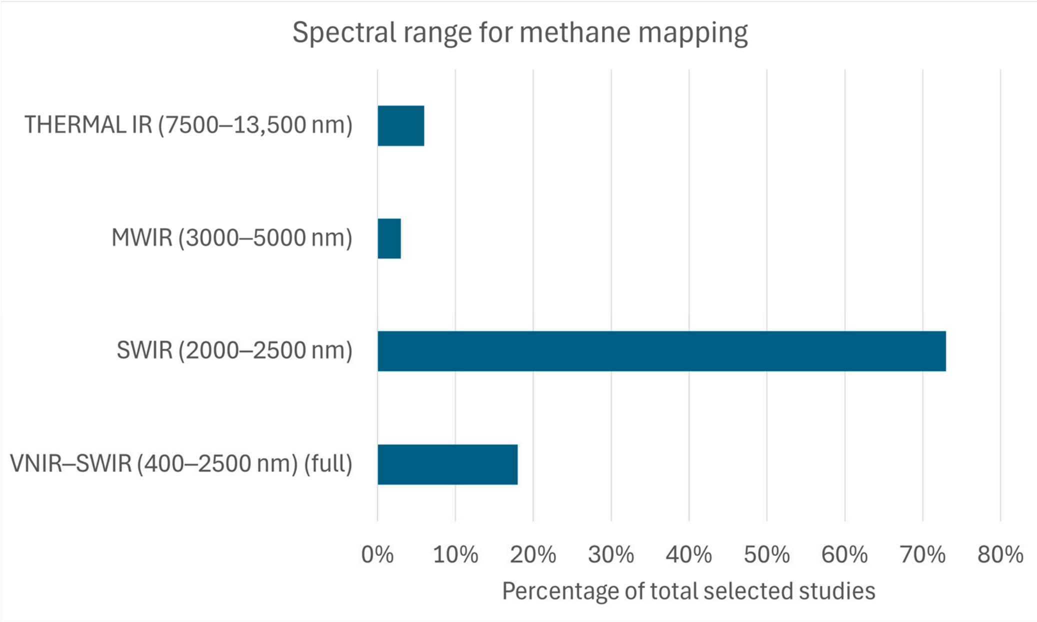

Figure 21. Spectral range used for methane mapping.

Analyzing the R^2 values reported across different categories (Figure 22), we see the following:

- Hybrid ML + RTM approaches show the highest maximum R^2 value ranges, between a minimum of 0.96 and a maximum of 0.99, confirming that integrating physics-based modeling with ML correction layers provides the most reliable methane retrievals.
- ML models, including tree-based and Boosting methods, show a constant range, from ~0.9 to ~0.92, depending heavily on feature engineering and background characterization.
- Deep learning models (CNNs, Siamese, Diffusion models), with R^2 from ~0.74 to ~0.85, show potential for plume detection but still struggle slightly with precise quantification compared to hybrid systems.
- C/PB methods explain that there is still a good option in methane mapping (~0.84 to ~0.99) but with higher variability, due to sensitivity to background spectral variability, atmospheric correction errors, and methane concentration levels.

6.3. Synthesis of Main Findings and Remaining Challenges

The results across the four products selected and across the two application domains reveal a consistent pattern about how algorithm classes are used and where their limitations arise. For vegetation products (CWC and CC), ML and DL methods dominate more than others and reach the highest R^2 values reported, but their performance strongly depends on data quality, field-based calibration and the availability of the full spectrum coverage (VNIR-SWIR). Hybrid models are used less but already show a notable balance between accuracy and robustness, especially when radiative transfer models (RTMs) are used to regularize ML estimators.

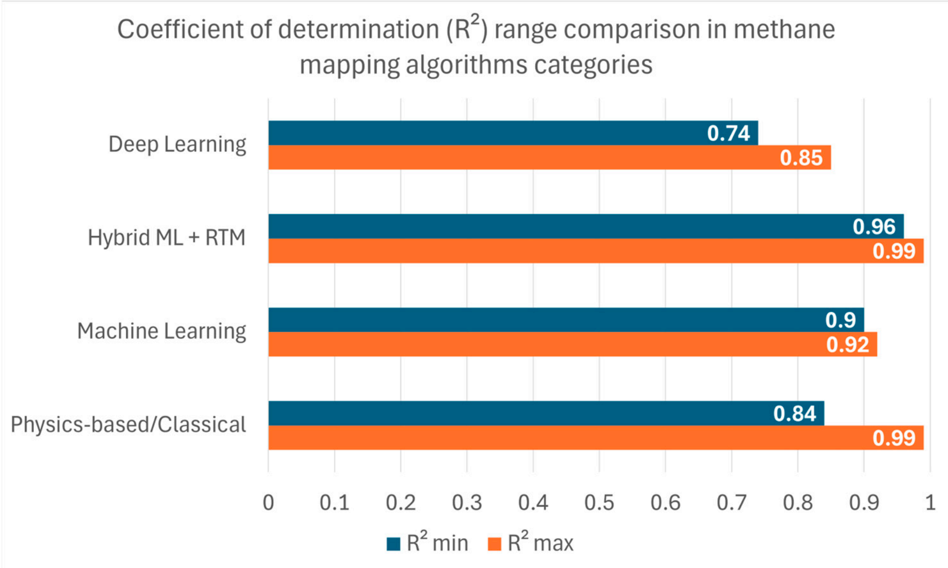

Figure 22. Coefficient of determination (R^2) range comparison in methane mapping algorithm categories. The blue bars indicate the minimum value of R2 reported, while the orange bars indicate the maximum value.

In the raw materials domain, C/PB methods remain strongly used and very effective, especially when spectral features are strong and pixels are relatively pure. ML and DL become more advantageous in heterogenous and mixed scenes. For methane, the current results confirm that C/PB approaches are still essential to exploit narrow absorption features under low-SNR conditions, while emergent methodology within DL and hybrid algorithms sections has been shown to reduce false positives and improve plume detection.

These insights highlight a set of cross-cutting challenges, data scarcity and representativeness, sensor limitations (spectral/spatial/temporal), and limited uncertainty reporting, which are repeatedly encountered across domains. In the following Discussion, we explicitly link these challenges to the algorithm groups reviewed and outline how classical, ML/DL and hybrid approaches can contribute to resolving them, also in view of upcoming missions such as CHIME, SBG and IRIDE.

7. Discussion

The analysis of 194 scientific papers on four key products (canopy water content, chlorophyll content, mineral presence maps, and methane detection) in two application domains (vegetation and raw materials) provides quantitative insight into the current state of the art of hyperspectral algorithms. The time range considered for the analysis ranges from 2015 and 2025, which coincides with the availability and consolidation of spaceborne and airborne hyperspectral sensors. This review supports the understanding of the most promising direction for the processing of hyperspectral data. Hyperspectral data analysis is constantly evolving, and machine learning (ML) and deep learning (DL) methods are increasingly central to operational applications. This review provides an understanding of the current algorithmic and sensor trends in hyperspectral data processing in Earth Observation, which are most relevant to the optics of new hyperspectral satellite missions such as CHIME (ESA), considering selected high-priority products (HPPs). As demonstrated by Berger et al. [17], the products here considered need further attention for increasing their TRLs, and this can be reached by exploring the synergy of future satellite missions, such as CHIME, Sentinel 2 Next Generation, and Copernicus Expansion missions. Rather than a simplistic description of the performance per single methodology, the results of this work highlight deeper patterns in how the domain of application, the typology of the sensor and the quality of the training and validation data all contribute to algorithm choice and, consequently, to the retrieval accuracy. Limitations of the review process include restriction to two scientific paper databases and the inclusion of only English, open access studies. Furthermore, studies that did not report quantitative accuracy metrics (e.g., R^2, RMSE or OA) were excluded during the eligibility screening stage.

Additionally, the synthesis of trends and results also reveals how specific classes of algorithms can be used to address important products within the selected application domain. In the following, we discuss not only where C/PB, ML/DL and hybrid approaches perform well or poorly but also how they can be combined or adapted to mitigate limitations related to spectral complexity, mixed pixels, sensor constraints and data availability.

7.1. Vegetation

The maturity of algorithms in the estimation of the CWC has progressed in a significant way, with ML emerging as a relevant methodology, used in 56% of the papers analyzed on this item. This reflects a consolidated use of data-driven approaches, supported by their ability to represent this kind of variable in the high-dimensional hyperspectral data, by considering the entire VNIR-SWIR range, which was used in more than 55% of study cases about CWC assessment [61].

Considering the ML algorithms, Boosting algorithms and tree-based ensembles (e.g., Random Forest, XGBoost) are most frequently applied, as well as GPR and SVM. These kinds of methodologies demonstrate strong capability to evaluate the CWC variable. Also, the performance varies significantly, indicating high potential, but it is also important considering the input data quality. Hybrid models (e.g., ML + RTM) are represented in 11% of cases, but they consistently achieve stable performance across studies. Their ability to integrate physical constraints from Radiative Transfer Models (RTMs) with the flexibility of ML makes them particularly promising for operational-scale applications, especially in satellite-based mapping of heterogeneous, mixed-vegetation canopies [62]. Several studies have demonstrated how hybrid strategies are able to blend the physics described by methodologies such as RTMs and use the efficiency of ML to infer vegetation variables such as the CWC, which are influenced mainly by spectral feature selection balanced with the signal-to-noise ratio for each hyperspectral band [14].

This is increasingly relevant, as upcoming missions, such as IRIDE and CHIME, aim to deliver global-scale, operational vegetation products. Conversely, physics-based models alone (e.g., RTMs, LUTs) show lower and more constrained accuracy, revealing their limitations in representing canopy heterogeneity and non-linear dynamics. C/PB approaches are mainly related to the regression relationship between field observation data and vegetation indices. This method is easy to use but is significantly dependent on the availability of observational data. Other relevant physical models are based on the response of CWC to canopy reflectance, by simplifying the simulation of solar radiation and the transfer processes. Also, in this case, the application of these models is limited by model parametrization [63]. Another relevant point to consider is the scale of the data and the type of data platform. High-performance models are generally developed using small-scale, homogeneous datasets, primarily based on field data collected using a spectroradiometer and a UAV with mounted hyperspectral sensors, where the signal quality and canopy condition are also controlled [62]. However, the extension of these models to spaceborne sensors (e.g., PRISMA, EnMAP, Sentinel-2) introduces relevant challenges, such as atmospheric effects, limitation of data availability for the area of interest (low revisit time) and low spatial resolution. These can impact model transferability.

These results suggest how combining RTM-based simulations or priors with ML models trained on multi-platform data (field, UAV, satellite) is relevant in the CWC analysis. RTMs can constrain the solution space and ensure physical consistency, while ML captures non-linear residuals and sensor-specific effects. This hybridization approach directly addresses the challenges of heterogeneity and sensor differences that are faced by purely physics-based or purely data-driven methods [14].

For the CC evaluation, ML is even more pronounced, used in 59% of the studies reviewed. It is underlined that chlorophyll has strong optical activity in the red-edge region [64]. In terms of algorithm performance, ML and DL models achieve the highest accuracy, improving the prediction accuracy of leaf chlorophyll content at different growth stages [65]. Tree-based ensemble models are the most applied from the ML family, followed by SVM and GPR. DL architectures (e.g., CNN) are represented in 12% of the cases, while for CWC, it is only 6%. This is due to the higher availability of reference datasets and well-characterized chlorophyll spectral responses [66]. Hybrid approaches (ML or DL combined with RTMs) are less present in the cases analyzed but demonstrate significant potential. These C/PB-informed ML models offer robustness in generalization, which is relevant in transferring models across different land cover categories and by using different sensor platforms [35,67]. They outperform purely physics-based models, which, while interpretable, often fail to capture subtle spectral variability, based on the papers selected, especially under heterogeneous conditions. Sensor platform analysis for CC reveals a predominance of field spectroradiometers and UAV-mounted hyperspectral sensors. This reflects the necessity of high-spatial-resolution data to resolve canopy-scale chlorophyll variability. The adoption of satellite sensors (e.g., PRISMA) is more frequent but still limited by requirements such as spectral resolution, limited revisit time for vegetation assessment in different seasons, and spatial resolution (30 m) and calibration uncertainties [68]. Spectral range utilization aligns closely with that of CWC, with >85% of studies employing the full VNIR-SWIR range. However, for chlorophyll specifically, the VNIR domain (400–1000 nm) is especially critical due to the concentration of diagnostic absorption features [66].

The reviewed studies indicate that physics-informed ML is effective in the stabilization of CC retrievals across sites and sensors. By using RTM simulations, red-edge band selection and chlorophyll-sensitive indices as priors or features [69], ML and DL models can reduce overfitting, improve interpretability and better handle spectral variability, thereby addressing one of the main challenges identified in the results: the limited transferability of purely empirical models [47].

7.2. Raw Materials

In the raw materials domain, mineral mapping from hyperspectral data presents a distinct methodological direction, reflecting both the complexity of mineralogical signatures and the maturity of traditional remote sensing techniques in this domain. The field still relies primarily on C/PB algorithms, particularly in scenarios with limited spatial extent and high mineral purity, such as airborne surveys targeting hydrothermal alteration zones or desert outcrops [70]. This heavy reliance on C/PB methods is justified by the strong diagnostic absorption features that minerals display in the VNIR-SWIR range, which have enabled high-accuracy mapping, without the need for complex learning models [71–73]. However, as the field shifts toward larger and more heterogeneous areas, with the presence of a high number of mixed pixels, especially with the rise of new spaceborne hyperspectral missions like PRISMA, the operational paradigm is evolving. In such contexts, C/PB methods often experience reduced performance due to spectral mixing and atmospheric variability. Consequently, ML and DL are becoming increasingly relevant, offering flexibility and automation to address these new challenges. Their adoption remains constrained by the need for high-quality, labeled ground-truth data, which are often limited in mineral exploration contexts [70]. Hybrid models, combining spectral matching with ML refinement, could offer the best trade-off between accuracy and robustness, though they are still emerging and underrepresented in current applications. In order to address the limitations of classical methods in heterogeneous mineral scenes, as evidenced by the results, a two-stage hybrid workflow is proposed. The workflow comprises the following stages: (1) physics-based spectral matching (e.g., SAM, MF, unmixing) for candidate detection and feature extraction, followed by (2) ML or DL classifiers operating on a reduced set of pixels and features. This strategy is predicated on the premise that it preserves the interpretability of C/PB methods while leveraging data-driven models to improve accuracy in mixed pixels and noisy conditions [74]. This is of particular importance for large-scale mapping with CHIME-like sensors such as EnMAP [46,47,75].

For the studies analyzed related to methane mapping, it remains predominantly rooted to C/PB algorithms, mostly related to the narrow and low SNR (signal–noise ratio) in the corresponding absorption features of this gas, which requires refined knowledge of the spectral behavior of the methane and the background normalization. Many of the study cases use airborne data (e.g., AVIRIS) and over high-flux leakage sources (e.g., on gas infrastructures or landfills), with plumes very extended in space and in clear contrast with the background [76]. DL models, particularly the ones that incorporate spatial learning (such as CNNs or Siamese networks), are emerging in the scientific literature, allowing for a relevant reduction in false positives and improving plume delineation. The ability of this kind of algorithm in methane quantification remains strictly connected and limited by the lack of validated datasets. The highest performances (R^2 near 0.99) in a few cases are related to the use of hybrid models, combining spectral matched filtering, with neural networks trained on real and synthetic data [57,77,78]. This methodology is represented only in 9% of the studies considered; the studies are limited in number, but they offer a scalable and transferable path in the optics of an operational CH_4 monitoring service in orbit. Overall, C/PB methods are relevant and still necessary in methane mapping, for precise SWIR real absorption assessment, but novel learning-based models progressively model hybridization, enhancing detection sensitivity and robustness, especially in noise handling in heterogeneous scenes.

In practical terms, this review suggests that methane mapping challenges can be addressed by combining the following: (1) physics-based SWIR matched filtering for robust detection of CH_4 absorption; (2) DL models that learn spatial plume coherence and background patterns; and (3) synthetic data generation to compensate for the scarcity of well-validated training datasets. This triad directly tackles the issues of low SNR, false positives and limited labelled data highlighted in the results [53,77,79].

7.3. Overall Discussion of the Main Findings and Challenges for Hyperspectral Applications

Beyond the discussion of specific application domains and products, the findings of this review highlighted common challenges for future hyperspectral applications.

Firstly, currently available hyperspectral sensor technical characteristics represent a constraint [7]. Across all the additional and high-priority products, performance is closely linked to the following:

- Spectral coverage: More than 70% of the studies require a full-range spectrum VNIR-SWIR (400–2500 nm), especially for vegetation assessment but also for mineral detection.
- Spatial resolution: Studies based on UAV and airborne data showed higher accuracy then the satellite-based ones. High-resolution datasets derived from these platforms

are relevant in supervised ML approaches such as SVM and RF but also in object-based classification methods, where additional spatial details improve mapping.
- Revisit time and multi-sensor approach: The existing hyperspectral sensors are limited in the revisit time and are not operational yet. This limits the possibility of time-series analysis and a multi-sensor approach. In fact, the number of studies implementing multi-temporal or multi-sensor approaches is very limited.

Future missions such as CHIME, SBG and IRIDE will help to reduce some of these limitations. Behind these, their benefits will be fulfilled only if algorithm development evolves. In fact, the development of a robust processing chain that integrates hybrid models can reduce the impact of the technical limits of these sensors, for example, to improve spatial or temporal resolution [80,81]. Within this landscape, hybrid approaches emerge as a particularly promising direction [82–85]. Physics-based components can introduce physical consistency, constrain the solution space and support the estimation of uncertainty, while ML/DL models can capture complex spectral–spatial patterns and integrate information from multiple sensors. In addition, recent Foundation Models (FMs), large-scale hyperspectral classification frameworks such as SpectralEarth, HyperSIGMA, and HyperSL, were not systematically reviewed, as they primarily target representation learning and specific classification benchmarks rather than product-specific variable retrieval; however, they represent a promising basis for future hyperspectral data processing [82–85].

Finally, our analysis revealed that differences in accuracy are also driven by ground-truth datasets. Studies with dense and well-distributed field data, derived from field campaigns, gauging stations or airborne campaigns, show higher product accuracy and higher algorithm robustness. This is particularly relevant in DL and in hybrid models, which require diverse training data to achieve generalization of the model. On the other side, models applied at local scale, with small training datasets, are limited in performance and generalizability [85]. This highlights the need for open benchmark datasets, Cal/Val infrastructures and shared and general validation protocols, especially in view of the new hyperspectral missions such as CHIME and IRIDE [41].

Taken together, these elements suggest three key priorities for future research: (1) the development of future and upcoming hyperspectral missions, such as CHIME and IRIDE (PLATiNO), should take into account the technical requirements to improve the image availability and quality; (2) it is necessary to develop and improve the design of physics-informed ML architectures that embed physics-based spectral references; and (3) it is necessary to enhance systematic field dataset construction for algorithm training and validation of the products. These findings are in line with the conclusion of a recent study by Berger et al. [17].

8. Conclusions and Future Research Directions

This review provides a comprehensive and comparative analysis of the main algorithmic strategies and sensor characteristics in hyperspectral data processing (across two application domains and four high-level products). These product categories, selected based on their alignment with CHIME's HPPs and additional products, are deeply connected to an emerging global need in environmental monitoring, sustainable resource management and climate policy frameworks, as highlighted in the Introduction.

While each of these products presents specific challenges and signal characteristics, several cross-cutting trends emerge that are particularly relevant in view of upcoming hyperspectral missions such as CHIME, SBG, and IRIDE [7].

A core finding is that a single category of algorithms (C/PB, ML, DL) cannot universally outperform others across all use cases. Instead, performance is strictly dependent on the physical properties of the target, data quality, data availability, scale, and the intended operational use. A relevant result is the growing importance of hybrid models, which combines the interpretability and transferability of the C/PB methods with the adaptability and automation of ML/DL. Although still underrepresented in the literature, these approaches are increasingly seen as the most promising for ensuring both robustness and scalability, two features that are essential for transitioning from research-grade analyses to operational services.

Across the different application domains, the use of ML/DL methods varies according to the specific study case. Applications involving high-dimensionality data and relevant spatial heterogeneity, such as the vegetation biophysical assessment, benefit more from ML/DL versatility. Instead, use cases involving well-characterized and specific spectral features, like pure mineral surfaces, are still relying on C/PB methods, which are still needed for these types of analysis. This uneven distribution of algorithmic needs reflects diverse user communities. These communities include research institutions seeking, for example, biophysical indicators. Resource management agencies need routine mineral monitoring. Climate-focused bodies are pushing for transparent, near-real-time methane assessments.

These results highlight an important shift: algorithm assessment and development are no longer purely related to the technical–scientific research field but increasingly driven by operational goals and policy frameworks. Documents, such as the European Green Deal, the Critical Raw Materials Act and the Global Methane Pledge, all point to EO, in particular to the new and high-potentiality sensors such as the hyperspectral ones, as a strategic enabler. In fact, in response to these needs, space agencies like ESA, NASA and ASI are designing new missions, such as CHIME, SBG and PLATiNO, from the IRIDE Constellation, with a relevant focus on algorithm maturity and an open access processing chain to support higher-level products based on that.

Based on the evidence gathered in this review, starting from the need for VNIR-SWIR full-spectral coverage to the impact of spatial resolution, revisit time, etc., to address these constraints, not only is an advancement in sensors and algorithms required but also a tailored and complementary muti-mission strategy.

In order to achieve success in present and future hyperspectral missions, it is essential to undertake a comprehensive evaluation of the various prospective research directions. This evaluation must encompass the development of hybrid processing chains, the enhancement of construction and the enhancement of availability of open training datasets, the establishment of a standardized accuracy assessment protocol, and the creation of interoperable architecture. These measures are imperative to ensure integration across a multitude of platforms and missions, including hyperspectral ones, thereby facilitating the development of a broad spectrum of multi-source operational services.

In this evolving landscape, it becomes clear that future success will not depend on replacing one class of methods with another. Instead, it will be achieved by bringing together the explanatory power of C/PB models and the flexibility of the ML/DL framework, guided by user needs and mission constraints. This convergence is not just a technical upgrade; it is a key pathway to unlock the full potential of hyperspectral data in support of environmental monitoring, resource security, climate action, policy implementation, scientific monitoring, and industrial innovation.

Supplementary Materials: The following supporting information can be downloaded at: https://www.mdpi.com/article/10.3390/rs18050798/s1, Table S1: Data-extraction template, listing the column names extracted during the screening phase.

Author Contributions: Conceptualization, A.T., S.L. and E.V.; methodology, S.L. and S.S.; formal analysis, S.L., S.S. and A.N.X.; investigation, A.T., S.L., A.N.X. and E.V.; resources, A.T., A.N.X., S.M. and E.V.; data curation, S.L.; writing—original draft preparation, S.L. and A.T.; writing—review and editing, S.L., A.N.X. and S.S.; visualization, S.L., A.N.X., S.M. and S.S.; supervision, A.T., E.V. and A.N.X.; project administration, A.T. and A.N.X.; funding acquisition, A.T. All authors have read and agreed to the published version of the manuscript.

Funding: This research was funded by the CHEES Chime End to End Mission Performance Simulator ISPRA-GMV Contract No. GMVAD CHEES/ISPRA 30747/22 and Space It Up project funded by the Italian Space Agency, ASI, and the Ministry of University and Research, MUR, under contract n. 2024-5-E.0-CUP n. I53D24000060005.

Institutional Review Board Statement: This review was not registered in PROSPERO or any other database, and no formal protocol was prepared.

Data Availability Statement: No original datasets or code were generated for this review. Extracted data tables used for analysis are available from the corresponding author upon reasonable request.

Acknowledgments: This paper and related research have been conducted during and with the support of the Italian national in-ter-university PhD course in Earth Observation of the University of Rome "Sapienza", co-funded by Scuola Universitaria Superiore (IUSS) of Pavia and by Aresys s.r.l.

Conflicts of Interest: Author Simone Mancon was employed by the company Aresys S.r.l. The remaining authors declare that the research was conducted in the absence of any commercial or financial relationships that could be construed as a potential conflict of interest.

References

1. Schodlok, M.C.; Frei, M.; Segl, K. Implications of new hyperspectral satellites for raw materials exploration. *Miner. Econ.* **2022**, *35*, 495–502. [CrossRef]
2. Inoue, Y.; Guérif, M.; Baret, F.; Skidmore, A.; Gitelson, A.; Schlerf, M.; Olioso, A. *Simple and Robust Methods for Remote Sensing of Canopy Chlorophyll Content: A Comparative Analysis of Hyperspectral Data for Different Types of Vegetation*; Wiley Online Library: Hoboken, NJ, USA, 2016. [CrossRef]
3. Owalekar, K.; Italia, U.; Vijeta; Deshpande, S. Comparative assessment of methane leak detection using hyperspectral data. In *Proceedings of the International Conference on Data Management, Analytics & Innovation*; Springer: Berlin, Germany, 2023; pp. 783–815.
4. Manolakis, D.; Truslow, E.; Pieper, M.; Cooley, T.; Brueggeman, M. Detection Algorithms in Hyperspectral Imaging Systems: An Overview of Practical Algorithms. *IEEE Signal Process. Mag.* **2014**, *31*, 24–33. [CrossRef]
5. Stanzione, V.; Contini, C.; Mafficini, A.; Novi, S.; Ficco, G.; Meini, M.; Mastrandrea, M.; Fidanzati, P.; Pulcino, V.; Ansalone, L. PLATiNO multimission platform for ESA (Italian PNRR) IRIDE hyperspectral optical mission. In *Proceedings of the Small Satellites Systems and Services Symposium (4S 2024)*; Petrozzi-Ilstad, M., Ed.; SPIE: Bellingham, WA, USA, 2025; p. 37. [CrossRef]
6. Ghamisi, P.; Yokoya, N.; Li, J.; Liao, W.; Liu, S.; Plaza, J.; Rasti, B.; Plaza, A. Advances in Hyperspectral Image and Signal Processing: A Comprehensive Overview of the State of the Art. *IEEE Geosci. Remote Sens. Mag.* **2017**, *5*, 37–78. [CrossRef]
7. Schiavon, E.; Taramelli, A.; Tornato, A.; Lee, C.M.; Luvall, J.C.; Schollaert Uz, S.; Townsend, P.A.; Cima, V.; Geraldini, S.; Nguyen Xuan, A.; et al. Maximizing Societal Benefit Across Multiple Hyperspectral Earth Observation Missions: A User Needs Approach. *J. Geophys. Res. Biogeosci.* **2023**, *128*, e2023JG007569. [CrossRef]
8. Cawse-Nicholson, K.; Townsend, P.A.; Schimel, D.; Assiri, A.M.; Blake, P.L.; Buongiorno, M.F.; Campbell, P.; Carmon, N.; Casey, K.A.; Correa Pabon, R.E.; et al. NASA's surface biology and geology designated observable: A perspective on surface imaging algorithms. *Remote Sens. Environ.* **2021**, *257*, 112349. [CrossRef]
9. Chakravarty, S.; Paikaray, B.K.; Mishra, R.; Dash, S. Hyperspectral Image Classification using Spectral Angle Mapper. In *Proceedings of the 2021 IEEE International Women in Engineering (WIE) Conference on Electrical and Computer Engineering (WIECON-ECE)*; IEEE: New York, NY, USA, 2021; pp. 87–90. [CrossRef]
10. Valentini, E.; Taramelli, A.; Marinelli, C.; Martin, L.P.; Fassari, M.; Troffa, S.; Mzid, N.; Casa, R.; Pignatti, S. Hyperspectral Mixture Models in the CHIME Mission Implementation for Topsoil Texture Retrieval. *J. Geophys. Res. Biogeosci.* **2023**, *128*, e2022JG007272. [CrossRef]
11. Shafri, H.Z.M. Machine Learning in Hyperspectral and Multispectral Remote Sensing Data Analysis. In *Artificial Intelligence Science and Technology*; World Scientific: Singapore, 2017; pp. 3–9. [CrossRef]
12. Hool, A.; Helbig, C.; Wierink, G. Challenges and opportunities of the European Critical Raw Materials Act. *Miner. Econ.* **2024**, *37*, 661–668. [CrossRef]

13. Malley, C.S.; Borgford-Parnell, N.; Haeussling, S.; Howard, I.C.; Lefèvre, E.N.; Kuylenstierna, J.C.I. A roadmap to achieve the global methane pledge. *Environ. Res. Clim.* **2023**, *2*, 011003. [CrossRef]
14. Pascual-Venteo, A.B.; Portalés, E.; Berger, K.; Tagliabue, G.; Garcia, J.L.; Pérez-Suay, A.; Rivera-Caceido, J.P.; Verrelst, J. Prototyping Crop Traits Retrieval Models for CHIME: Dimensionality Reduction Strategies Applied to PRISMA Data. *Remote Sens.* **2022**, *14*, 2448. [CrossRef]
15. European Space Agency and Copernicus. Copernicus Hyperspectral Imaging Mission for the Environment Mission Requirements Document, ESA-EOPSM-CHIM-MRD-3216, Version 3.0. 2021. Available online: https://sentiwiki.copernicus.eu/__attachments/1678167/ESA-EOPSM-CHIM-MRD-3216%20-%20Copernicus%20Hyperspectral%20Imaging%20Mission%20for%20the%20Environment%20MRD%202021%20-%203.0.pdf?inst-v=19224347-b78a-4e98-8878-0bb2ef5b4589 (accessed on 15 January 2024).
16. Taramelli, A.; Tornato, A.; Magliozzi, M.L.; Mariani, S.; Valentini, E.; Zavagli, M.; Costantini, M.; Nieke, J.; Adams, J.; Rast, M. An interaction methodology to collect and assess user-driven requirements to define potential opportunities of future hyperspectral imaging sentinel mission. *Remote Sens.* **2020**, *12*, 1286. [CrossRef]
17. Berger, K.; Hostert, P.; Schlerf, M.; Immitzer, M.; Szantoi, Z.; Okujeni, A.; Foerster, S.; Colditz, R.; Giardino, C.; Machwitz, M.; et al. Advancing optical earth observation for EU policies: Needs, opportunities, recommendations. *Environ. Sci. Eur.* **2026**, *38*, 52. [CrossRef]
18. Matemilola, S.; Fadeyi, O.; Sijuade, T. Paris agreement. In *Encyclopedia of Sustainable Management*; Springer International Publishing: Cham, Switzerland, 2023; pp. 2555–2559. [CrossRef]
19. Chiu, I.H.Y. The EU sustainable finance agenda: Developing governance for double materiality in sustainability metrics. *Eur. Bus. Organ. Law Rev.* **2022**, *23*, 87–123. [CrossRef]
20. Shaik, R.U.; Periasamy, S.; Zeng, W.P. Potential Assessment of PRISMA Hyperspectral Imagery for Remote Sensing Applications. *Remote Sens.* **2023**, *15*, 1378. [CrossRef]
21. Van der Meer, F.D.; Van der Werff, H.M.; Van Ruitenbeek, F.J.; Hecker, C.A.; Bakker, W.H.; Noomen, M.F.; Van der Meijde, M.; Carranza, E.J.M.; De Smeth, J.B.; Woldai, T. Multi-and hyperspectral geologic remote sensing: A review. *Int. J. Appl. Earth Obs. Geoinf.* **2012**, *14*, 112–128. [CrossRef]
22. Kumar, S.; Arevalo, I.; Manjunath, B.S. Methane Mapper: Spectral Absorption Aware Hyperspectral Transformer for Methane Detection. Available online: https://github.com/UCSB-VRL/MethaneMapper-Spectral-Absorption-aware-Hyperspectral-Transformer-for-Methane-Detection (accessed on 5 November 2024).
23. Yang, G.; Huang, K.; Sun, W.; Meng, X.; Mao, D.; Ge, Y. Enhanced mangrove vegetation index based on hyperspectral images for mapping mangrove. *ISPRS J. Photogramm. Remote Sens.* **2022**, *189*, 236–254. [CrossRef]
24. Qian, S.-E. Hyperspectral Satellites, Evolution, and Development History. *IEEE J. Sel. Top. Appl. Earth Obs. Remote Sens.* **2021**, *14*, 7032–7056. [CrossRef]
25. Jia, J.; Wang, Y.; Chen, J.; Guo, R.; Shu, R.; Wang, J. Status and application of advanced airborne hyperspectral imaging technology: A review. *Infrared Phys. Technol.* **2020**, *104*, 103115. [CrossRef]
26. Adão, T.; Hruška, J.; Pádua, L.; Bessa, J.; Peres, E.; Morais, R.; Sousa, J.J. Hyperspectral imaging: A review on UAV-based sensors, data processing and applications for agriculture and forestry. *Remote Sens.* **2017**, *9*, 1110. [CrossRef]
27. Benelli, A.; Cevoli, C.; Fabbri, A. In-field hyperspectral imaging: An overview on the ground-based applications in agriculture. *J. Agric. Eng.* **2020**, *51*, 129–139. [CrossRef]
28. Aburaed, N.; Alkhatib, M.Q.; Marshall, S.; Zabalza, J.; Al Ahmad, H. A Review of Spatial Enhancement of Hyperspectral Remote Sensing Imaging Techniques. *IEEE J. Sel. Top. Appl. Earth Obs. Remote Sens.* **2023**, *16*, 2275–2300. [CrossRef]
29. Neinavaz, E.; Schlerf, M.; Darvishzadeh, R.; Gerhards, M.; Skidmore, A.K. Thermal infrared remote sensing of vegetation: Current status and perspectives. *Int. J. Appl. Earth Obs. Geoinf.* **2021**, *102*, 102415. [CrossRef]
30. Lee, C.M.; Glenn, N.F.; Stavros, E.N.; Luvall, J.; Yuen, K.; Hain, C.; Schollaert Uz, S. Systematic integration of applications into the Surface Biology and Geology (SBG) Earth mission architecture study. *J. Geophys. Res. Biogeosci.* **2022**, *127*, e2021JG006720. [CrossRef]
31. Rao, D.A.; Guha, A. Potential Utility of Spectral Angle Mapper and Spectral Information Divergence Methods for mapping lower Vindhyan Rocks and Their Accuracy Assessment with Respect to Conventional Lithological Map in Jharkhand, India. *J. Indian Soc. Remote Sens.* **2018**, *46*, 737–747. [CrossRef]
32. Gomez, C.; Lagacherie, P.; Coulouma, G. Continuum removal versus PLSR method for clay and calcium carbonate content estimation from laboratory and airborne hyperspectral measurements. *Geoderma* **2008**, *148*, 141–148. [CrossRef]
33. Liu, H.; Li, W.; Xia, X.-G.; Zhang, M.; Guo, Z.; Song, L. SegHSI: Semantic Segmentation of Hyperspectral Images with Limited Labeled Pixels. *IEEE Trans. Image Process.* **2024**, *33*, 6469–6482. [CrossRef] [PubMed]
34. Kumar, V.; Venkatachalaperumal, S.R.; Persello, C. Synergistic fusion of spaceborne polarimetric SAR and hyperspectral data for land cover classification. In *Spaceborne Synthetic Aperture Radar Remote Sensing*; CRC Press: Boca Raton, FL, USA, 2023; pp. 169–209.

35. Righini, M.; Valentini, E.; Sapio, S.; Marinelli, C.; Gatti, I.; Jimenez, M.J.; Bresciani, M.; Giardino, C.; Pinardi, M.; Boschetti, M.; et al. Dynamic land cover mapping exploiting hyperspectral PRISMA data. In *Proceedings of the IEEE International Geoscience and Remote Sensing Symposium (IGARSS 2023)*; IEEE: New York, NY, USA, 2023; pp. 1497–1500.
36. Rast, M.; Nieke, J.; Adams, J.; Isola, C.; Gascon, F. Copernicus Hyperspectral Imaging Mission for the Environment (CHIME). In *Proceedings of the International Geoscience and Remote Sensing Symposium (IGARSS)*; Institute of Electrical and Electronics Engineers Inc.: New York, NY, USA, 2021; pp. 108–111. [CrossRef]
37. Nieke, J.; Despoisse, L.; Gabriele, A.; Weber, H.; Strese, H.; Ghasemi, N.; Gascon, F.; Alonso, K.; Boccia, V.; Tsonevska, B.; et al. The Copernicus Hyperspectral Imaging Mission for the Environment (CHIME): An overview of its mission, system and planning status. In *Sensors, Systems, and Next-Generation Satellites XXVII*; SPIE: Bellingham, WA, USA, 2023; Volume 12729, pp. 21–40. [CrossRef]
38. Im, J.; Jensen, J.R. Hyperspectral Remote Sensing of Vegetation. *Geogr. Compass* **2008**, *2*, 1943–1961. [CrossRef]
39. Räsänen, A.; Aurela, M.; Juutinen, S.; Kumpula, T.; Lohila, A.; Penttilä, T.; Virtanen, T. Detecting northern peatland vegetation patterns at ultra-high spatial resolution. *Remote Sens. Ecol. Conserv.* **2020**, *6*, 457–471. [CrossRef]
40. Bian, L.; Wang, Z.; Zhang, Y.; Li, L.; Zhang, Y.; Yang, C.; Fang, W.; Zhao, J.; Zhu, C.; Meng, Q.; et al. A broadband hyperspectral image sensor with high spatio-temporal resolution. *Nature* **2024**, *635*, 73–81. [CrossRef] [PubMed]
41. Boccia, V.; Adams, J.; Thome, K.J.; Turpie, K.R.; Kokaly, R.; Bouvet, M.; Green, R.O.; Rast, M. NASA–ESA cooperation on the SBG and CHIME hyperspectral satellite missions: A roadmap for the Joint Working Group on Cal/Val activities. In *EGU General Assembly 2021, Conference Abstracts*; European Geosciences Union: Vienna, Austria, 2021; p. EGU21-15166. [CrossRef]
42. Pearlshtien, D.H.; Pignatti, S.; Ben-Dor, E. Vicarious CAL/VAL Approach for Orbital Hyperspectral Sensors Using Multiple Sites. *Remote Sens.* **2023**, *15*, 771. [CrossRef]
43. Bioucas-Dias, J.M.; Plaza, A.; Camps-Valls, G.; Scheunders, P.; Nasrabadi, N.; Chanussot, J. Hyperspectral Remote Sensing Data Analysis and Future Challenges. *IEEE Geosci. Remote Sens. Mag.* **2013**, *1*, 6–36. [CrossRef]
44. Habashi, J.; Moghadam, H.J.; Oskouei, M.M.; Pour, A.B.; Hashim, M. PRISMA Hyperspectral Remote Sensing Data for Mapping Alteration Minerals in Sar-e-Châh-e-Shur Region, Birjand, Iran. *Remote Sens.* **2024**, *16*, 1277. [CrossRef]
45. Green, R.O.; Mahowald, N.; Ung, C.; Thompson, D.R.; Bator, L.; Bennett, M.; Bernas, M.; Blackway, N.; Bradley, C.; Cha, J.; et al. The Earth Surface Mineral Dust Source Investigation: An Earth science imaging spectroscopy mission. In *Proceedings of the 2020 IEEE Aerospace Conference, Big Sky, MT, USA, 7-14 March 2020*; IEEE: New York, NY, USA, 2020; pp. 1–15. [CrossRef]
46. Pearlshtien, D.H.; Pignatti, S.; Greisman-Ran, U.; Ben-Dor, E. PRISMA sensor evaluation: A case study of mineral mapping performance over Makhtesh Ramon, Israel. *Int. J. Remote Sens.* **2021**, *42*, 5884–5916. [CrossRef]
47. Peyghambari, S.; Zhang, Y. Hyperspectral remote sensing in lithological mapping, mineral exploration, and environmental geology: An updated review. *J. Appl. Remote Sens.* **2021**, *15*, 031501. [CrossRef]
48. Asadzadeh, S.; Zhou, X.D.; Chabrillat, S. Assessment of the spaceborne EnMAP hyperspectral data for alteration mineral mapping: A case study of the Reko Diq porphyry Cu-Au deposit, Pakistan. *Remote Sens. Environ.* **2024**, *314*, 114389. [CrossRef]
49. Hajaj, S.; El Harti, A.; Pour, A.B.; Jellouli, A.; Adiri, Z.; Hashim, M. A review on hyperspectral imagery application for lithological mapping and mineral prospecting: Machine learning techniques and future prospects. *Remote Sens. Appl.* **2024**, *35*, 101218. [CrossRef]
50. Udelhoven, T.; Schlerf, M.; Segl, K.; Mallick, K.; Bossung, C.; Retzlaff, R.; Rock, G.; Fischer, P.; Müller, A.; Storch, T.; et al. A satellite-based imaging instrumentation concept for hyperspectral thermal remote sensing. *Sensors* **2017**, *17*, 1542. [CrossRef]
51. Vicente, L.E.; de Souza, C.R. Identification of mineral components in tropical soils using reflectance spectroscopy and advanced spaceborne thermal emission and reflection radiometer (ASTER) data. *Remote Sens. Environ.* **2011**, *115*, 1824–1836. [CrossRef]
52. Gålfalk, M.; Olofsson, G.; Bastviken, D. Approaches for hyperspectral remote flux quantification and visualization of GHGs in the environment. *Remote Sens. Environ.* **2017**, *191*, 81–94. [CrossRef]
53. Jiang, Y.; Zhang, L.; Zhang, X.; Cao, X. Methane Retrieval Algorithms Based on Satellite: A Review. *Atmosphere* **2024**, *15*, 449. [CrossRef]
54. Xiao, C.; Fu, B.; Shui, H.; Guo, Z.; Zhu, J. Detecting the Sources of Methane Emission from Oil Shale Mining and Processing Using Airborne Hyperspectral Data. *Remote Sens.* **2020**, *12*, 537. [CrossRef]
55. Dennison, P.E.; Thorpe, A.K.; Pardyjak, E.R.; Roberts, D.A.; Qi, Y.; Green, R.O.; Bradley, E.S.; Funk, C.C. High spatial resolution mapping of elevated atmospheric carbon dioxide using airborne imaging spectroscopy: Radiative transfer modeling and power plant plume detection. *Remote Sens. Environ.* **2013**, *139*, 116–129. [CrossRef]
56. Xu, D.Q.; Ni, G.Q.; Jiang, L.L.; Shen, Y.T.; Li, T.; Ge, S.L.; Shu, X.B. Exploring for natural gas using reflectance spectra of surface soils. *Adv. Space Res.* **2008**, *41*, 1800–1817. [CrossRef]
57. Ayasse, A.K.; Dennison, P.E.; Foote, M.; Thorpe, A.K.; Joshi, S.; Green, R.O.; Duren, R.M.; Thompson, D.R.; Roberts, D.A. Methane mapping with future satellite imaging spectrometers. *Remote Sens.* **2019**, *11*, 3054. [CrossRef]

58. Thorpe, A.K.; Roberts, D.A.; Bradley, E.S.; Funk, C.C.; Dennison, P.E.; Leifer, I. High resolution mapping of methane emissions from marine and terrestrial sources using a Cluster-Tuned Matched Filter technique and imaging spectrometry. *Remote Sens. Environ.* **2013**, *134*, 305–318. [CrossRef]
59. Gewali, U.B.; Monteiro, S.T.; Saber, E. Machine learning based hyperspectral image analysis: A survey. *arXiv* **2018**, arXiv:1802.08701.
60. Sr, W.L.S.; Revercomb, H.E.; Zhou, D.K.; Huang, H.-L.A. Hyperspectral sounding: A revolutionary advance in atmospheric remote sensing. In *Multispectral and Hyperspectral Remote Sensing Instruments and Applications II*; SPIE: Bellingham, WA, USA, 2005; pp. 1–11.
61. Wijesingha, J.; Dayananda, S.; Wachendorf, M.; Astor, T. Comparison of Spaceborne and UAV-Borne Remote Sensing Spectral Data for Estimating Monsoon Crop Vegetation Parameters. *Sensors* **2021**, *21*, 2886. [CrossRef] [PubMed]
62. Zhu, J.; Lu, J.; Li, W.; Wang, Y.; Jiang, J.; Cheng, T.; Zhu, Y.; Cao, W.; Yao, X. Estimation of canopy water content for wheat through combining radiative transfer model and machine learning. *Field Crops Res.* **2023**, *302*, 109077. [CrossRef]
63. Liu, L.; Li, S.; Yang, W.; Wang, X.; Luo, X.; Ran, P.; Zhang, H. Forest canopy water content monitoring using radiative transfer models and machine learning. *Forests* **2023**, *14*, 1418. [CrossRef]
64. Yang, X.; Yu, Y.; Fan, W. Chlorophyll content retrieval from hyperspectral remote sensing imagery. *Environ. Monit. Assess.* **2015**, *187*, 456. [CrossRef]
65. Ta, N.; Chang, Q.; Zhang, Y. Estimation of Apple Tree Leaf Chlorophyll Content Based on Machine Learning Methods. *Remote Sens.* **2021**, *13*, 3902. [CrossRef]
66. Clevers, J.G.; Kooistra, L. Using hyperspectral remote sensing data for retrieving canopy chlorophyll and nitrogen content. *IEEE J. Sel. Top. Appl. Earth Obs. Remote Sens.* **2011**, *5*, 574–583. [CrossRef]
67. Valentini, E.; Nghiem, S.V.; Thy, P.T.M.; Sapio, S.; Bresciani, M.; Giardino, C.; Boschetti, M.; Nutini, F.; Pellegrino, A.; Le Trung, C.; et al. Multisensor mapping of land use/land cover pattern in mangrove ecosystems: A case study in Cần Giờ Biosphere Reserve, Vietnam. *IEEE J. Sel. Top. Appl. Earth Obs. Remote Sens.* **2025**, *18*, 20776–20789. [CrossRef]
68. De Luca, G.; Carotenuto, F.; Genesio, L.; Pepe, M.; Toscano, P.; Boschetti, M.; Miglietta, F.; Gioli, B. Improving PRISMA hyperspectral spatial resolution and geolocation by using Sentinel-2: Development and test of an operational procedure in urban and rural areas. *ISPRS J. Photogramm. Remote Sens.* **2024**, *215*, 112–135. [CrossRef]
69. Wocher, M.; Berger, K.; Danner, M.; Mauser, W.; Hank, T. RTM-based dynamic absorption integrals for the retrieval of biochemical vegetation traits. *Int. J. Appl. Earth Obs. Geoinf.* **2020**, *93*, 102219.
70. Chen, X.; Warner, T.A.; Campagna, D.J. Integrating visible, near-infrared and short-wave infrared hyperspectral and multispectral thermal imagery for geological mapping at Cuprite, Nevada: A rule-based system. *Int. J. Remote Sens.* **2010**, *31*, 1733–1752. [CrossRef]
71. Kopačková, V.; Koucká, L. Integration of Absorption Feature Information from Visible to Longwave Infrared Spectral Ranges for Mineral Mapping. *Remote Sens.* **2017**, *9*, 1006. [CrossRef]
72. Johnson, K.E.; Koperski, K. VNIR-SWIR Superspectral Mineral Mapping: An Example from Cuprite, Nevada. *Photogramm. Eng. Remote Sens.* **2020**, *86*, 695–700. [CrossRef]
73. Koirala, B.; Khodadadzadeh, M.; Contreras, C.; Zahiri, Z.; Gloaguen, R.; Scheunders, P. A Supervised Method for Nonlinear Hyperspectral Unmixing. *Remote Sens.* **2019**, *11*, 2458. [CrossRef]
74. Adep, R.N.; Vijayan, A.P.; Shetty, A.; Ramesh, H. Performance evaluation of hyperspectral classification algorithms on AVIRIS mineral data. *Perspect. Sci.* **2016**, *8*, 722–726. [CrossRef]
75. Frankenberg, C.; Thorpe, A.K.; Thompson, D.R.; Hulley, G.; Kort, E.A.; Vance, N.; Borchardt, J.; Krings, T.; Gerilowski, K.; Sweeney, C.; et al. Airborne methane remote measurements reveal heavy-tail flux distribution in Four Corners region. *Proc. Natl. Acad. Sci. USA* **2016**, *113*, 9734–9739. [CrossRef]
76. Pieper, M.L.; Lockwood, R.; Chrisp, M. Hyperspectral SWIR sensor parameterization for optimal methane detection. In *Imaging Spectrometry XXVI: Applications, Sensors, and Processing*; SPIE: Bellingham, WA, USA, 2023; pp. 112–127.
77. Masiello, G.; Mastro, P.; Serio, C.; Falabella, F.; Pasquariello, P. Methane profile retrieval from IASI: A deep learning inversion approach based on feed-forward neural networks. In *Remote Sensing of Clouds and the Atmosphere XXVII*; Comerón, A., Kassianov, E.I., Schäfer, K., Picard, R.H., Weber, K., Singh, U.N., Eds.; SPIE: Bellingham, WA, USA, 2022; p. 10. [CrossRef]
78. Guanter, L.; Irakulis-Loitxate, I.; Gorroño, J.; Sánchez-García, E.; Cusworth, D.H.; Varon, D.J.; Cogliati, S.; Colombo, R. Mapping methane point emissions with the PRISMA spaceborne imaging spectrometer. *Remote Sens. Environ.* **2021**, *265*, 112671. [CrossRef]
79. Li, T.; Liu, T.; Wang, Y.; Li, X.; Gu, Y. Spectral Reconstruction Network from Multispectral Images to Hyperspectral Images: A Multitemporal Case. *IEEE Trans. Geosci. Remote Sens.* **2022**, *60*, 5535016. [CrossRef]
80. Muhammad, U.; Laaksonen, J. Hybrid Deep Learning for Hyperspectral Single-Image Super-Resolution. *IEEE Geosci. Remote Sens. Lett.* **2025**, *22*, 5509905. [CrossRef]
81. Yang, J.; Wu, C.; Du, B.; Zhang, L. Enhanced Multiscale Feature Fusion Network for HSI Classification. *IEEE Trans. Geosci. Remote Sens.* **2021**, *59*, 10328–10347. [CrossRef]

82. Wang, D.; Hu, M.; Jin, Y.; Miao, Y.; Yang, J.; Xu, Y.; Qin, X.; Ma, J.; Sun, L.; Li, C.; et al. HyperSIGMA: Hyperspectral Intelligence Comprehension Foundation Model. *IEEE Trans. Pattern Anal. Mach. Intell.* **2025**, *47*, 6427–6444. [CrossRef]
83. Li, J.; Liu, Y.; Wang, X.; Peng, Y.; Sun, C.; Wang, S.; Sun, Z.; Ke, T.; Jiang, X.; Lu, T.; et al. HyperFree: A channel-adaptive and tuning-free foundation model for hyperspectral remote sensing imagery. In *Proceedings of the IEEE/CVF Conference on Computer Vision and Pattern Recognition (CVPR 2025)*; IEEE: New York, NY, USA, 2025; pp. 23048–23058.
84. Yang, J.; Du, B.; Zhang, L. From center to surrounding: An interactive learning framework for hyperspectral image classification. *ISPRS J. Photogramm. Remote Sens.* **2023**, *197*, 145–166. [CrossRef]
85. Li, S.; Hao, Q.; Gao, G.; Kang, X. The Effect of Ground Truth on Performance Evaluation of Hyperspectral Image Classification. *IEEE Trans. Geosci. Remote Sens.* **2018**, *56*, 7195–7206. [CrossRef]